5-2012

Heater Geometry and Heat Flux Effects On Subcooled, Thin Wire, Nucleate Pool Boiling In Microgravity

Troy Munro
Utah State University

HEATER GEOMETRY AND HEAT FLUX EFFECTS ON SUBCOOLED, THIN WIRE, NUCLEATE POOL BOILING IN MICROGRAVITY

by

Troy Munro

A thesis submitted in partial fulfillment
of the requirements for the degree

of

MASTER OF SCIENCE

in

Mechanical Engineering

Approved:

_____	_____
Dr. Heng Ban Major Professor	Dr. John Robert Dennison Committee Member
_____	_____
Dr. Barton Smith Committee Member	Dr. Mark R. McLellan Vice President for Research and Dean of the School of Graduate Studies

UTAH STATE UNIVERSITY
Logan, Utah

2012

ABSTRACT

Heater Geometry and Heat Flux Effects on Subcooled, Thin Wire,

Nucleate Pool Boiling in Microgravity

by

Troy R. Munro, Master of Science

Utah State University, 2012

Major Professor: Dr. Heng Ban
Department: Mechanical and Aerospace Engineering

Nucleate boiling is widely used as a means of heat transfer in thermal management systems because of its high heat transfer rates. This study explored the effects of heat flux and surface geometry on heat transfer behavior and bubble dynamics of nucleate pool boiling in microgravity. A single platinum wire, a twist of three platinum wires, and a twist of four platinum wires were used as boiling surfaces for two separate experiments performed in microgravity on board NASA's parabolic flight aircraft. Wire temperature, thermocouple, and video measurements were taken during a total of 44 microgravity parabolas. Results show that the crevices formed by wire twisting provide regions of localized superheating and are able to reduce the heat flux necessary for boiling onset to occur. This localized heating results in a lower average heater temperature and shortened superheating periods, but this effect decreases when more wires are present in the twist. This behavior was investigated and confirmed with a finite volume, transient conduction model. This model also showed that the water temperature profile at the bubble onset indicates that water at a certain distance from the wire surface, in this experiment 50 μm, needs to be

heated to above saturation temperature in order to initiate and generate a burst of bubbles. A relative bubble area analysis method was able to quantify vapor production and bubble behavior across multiple frames of video. Application of this method revealed a transition of bubble behavior from large isolated bubbles to jet flows of small bubbles, and this method allowed the heat flux contribution of jet flows to be approximated. Additionally, a new mode of jet flows was observed. Particle image velocimetry was used to provide approximate velocities of small bubble jet flows and their influence on heat transfer to the bulk fluid.

(89 pages)

PUBLIC ABSTRACT

Heater Geometry and Heat Flux Effects on Subcooled, Thin Wire, Nucleate Pool Boiling in Microgravity

The purpose of this thesis is to study the effects of microgravity, surface geometry, and heat dissipation per unit area (heat flux) on boiling heat transfer. Boiling is able to move a significant amount of heat for a small area in comparison to other heat transfer methods. Space systems could benefit from the development of thermal management systems that use boiling heat transfer because they would be smaller, more robust, and less expensive. However, boiling is an extremely complicated process which has no comprehensive models to predict its behavior. Multiple correlations have been developed which relate heat transfer efficiencies to various system parameters, but they can only be applied to specific heat transfer systems, lack considerations for the actual mechanisms involved in boiling, and give erroneous results if used beyond their limited applications.

This research concluded that twisting thin wire heaters creates crevices that reduce the amount of heat needed to make the system boil. This is particularly beneficial in microgravity because heat transfer prior to boiling is very inefficient. Additionally, this study characterized the observation of a new mode of jet flows, which results in many small bubbles leaving the wire and creates a fluid flow that would not normally exist in microgravity. The results of this study show that sustained boiling can exist in microgravity and in some instances can be more effective than boiling in terrestrial gravity.

To my parents for teaching me the importance of education, and to Michaelene, Kaylee, and future baby brother who make it all worth it.

ACKNOWLEDGMENTS

First I would like to express my thanks to my major professor, Dr. Ban, for all his help and guidance through the many years of this project. His help and the help of Get Away Special (GAS) team mentors Dr. Jan Sojka and Dr. JR Dennison have guided me to become the researcher I am today.

Without the contributions of members of the GAS team, the two experiments that provided data for this thesis would never have gotten off the ground, literally. Special thanks are deserved to Andrew Fassmann, Justin Koeln, and Rob Barnett, who became my close friends and extensions of my brain through the design and analysis of both experiments. I could not have done this without them. I would like to also thank Dr. Doran Baker for supplying funding through the Rocky Mountain NASA Space Grant Consortium. Additional funding was also provided by SpaceX, Space Dynamics Laboratory, and National Instruments.

Finally, I would like to thank my family. My parents instilled in me the importance of education and encouraged me to do my best. My wife, Michaelene, and daughter Kaylee have been there for me every day along this journey, and I know they will be there the rest of the way. And I thank the Lord who has given me strength to do all things.

Troy R. Munro

CONTENTS

LIST OF TABLES

LIST OF FIGURES

NOMENCLATURE

Bi	Biot number
CHF	critical heat flux
h	heat transfer coefficient
k	thermal conductivity
L_{cr}	critical length
$\overline{Nu}_D$	average Nusselt number
ONB	onset of nucleate boiling
PIV	particle image velocimetry
Pr	Prandlt number
q''	heat flux
q'''	volumetric heat generation
q_0''	nominal heat flux
r_0	radius of wire
Re_D	Reynolds number
RTD	resistance temperature device
t	time
T	temperature
T_c	critical temperature of fluid
T_{cr}	critical temperature
T_s	surface temperature
T_∞	bulk fluid temperature
TC	thermocouple

$\Delta T_{sat,\ wire}$	difference of wire temperature from saturation temperature
$T_{surface}$	temperature of heater surface

Greek symbols

α	thermal diffusivity
ε	perturbation parameter
μ	dynamic viscosity of fluid
μ_s	dynamic viscosity of fluid at surface temperature
τ	time constant

Subscripts

μg	microgravity
1g	Earth's gravity
i	horizontal array index
j	vertical array index
wire	heater wire
le	large bubble boiling
se	small bubble boiling
sat	saturation

Superscripts

n	current frame number
initial	initial frame number

CHAPTER 1

INTRODUCTION

1.1. Introduction to Boiling Heat Transfer

Boiling research is a very important topic because of the high heat transfer rates and wide applicability in power generation and thermal management systems. As a convective method of heat transfer, the behavior and effectiveness of boiling of a wire heating element emerged in a fluid can be studied empirically through Newton's law of cooling, Eq. (1).

$$q" = h(T_{surface} - T_{fluid}) \tag{1}$$

where $q"$ is the heat per unit area (heat flux), $T_{surface}$ is the average temperature of the heater, T_{fluid} is the bulk temperature of the fluid, and h is the heat transfer coefficient. This heat transfer coefficient is of great importance and is the focus of many experiments and correlations because it is a representation of the magnitude of heat transfer for a given system. However, there is a need to understand the mechanisms and processes involved in boiling so that heat transfer characteristics can be better predicted - especially for use in space applications - without the need to perform experiments to determine the heat transfer coefficient for each system.

Straub has spent many decades investigating boiling behavior in microgravity and presents an excellent summary on the subject [1]. His justification for use of a microgravity environment is that reducing buoyancy effects allows the fundamental mechanisms to be studied and the self-induced dynamics of vapor bubbles in the absence of external forces to be viewed. To provide a microgravity environment for testing, Straub used ballistic rockets which achieve residual accelerations of 10^{-4} g, orbital flights through the Space Shuttle (through NASA's GetAway Special program) which achieve residual accelerations of 10^{-5} g, and aircraft flying in parabolic arcs which achieve residual accelerations of about 10^{-2} g. Because of the ease and availability of

parabolic aircraft use, the current study uses this method to simulate a microgravity environment, although the design of the hardware is based on results from an experiment performed on the Space Shuttle [2].

The results from Straub's experiments [1] have shown that sustained saturated pool boiling, where the bulk fluid is at saturation temperature, is possible in microgravity and in some instances, can experience higher heat transfer coefficients than terrestrial conditions. Additionally, bubble departure processes, such as coalescence and bubble ripening, can be attributed to surface tension effects in the absence of buoyancy forces. In subcooled boiling, where the bulk fluid is below saturation temperature, these surface tension effects are manifest in Marangoni flows (or thermocapillary flows shown in Figure 1-1) that are also able to transport heat to the bulk fluid but provide no heat transfer enhancement in comparison to saturated boiling. Straub's experiments have led him to the conclusion that the primary mechanism for heat transfer in boiling is evaporation in the microlayer, which exists between the bubble and heater

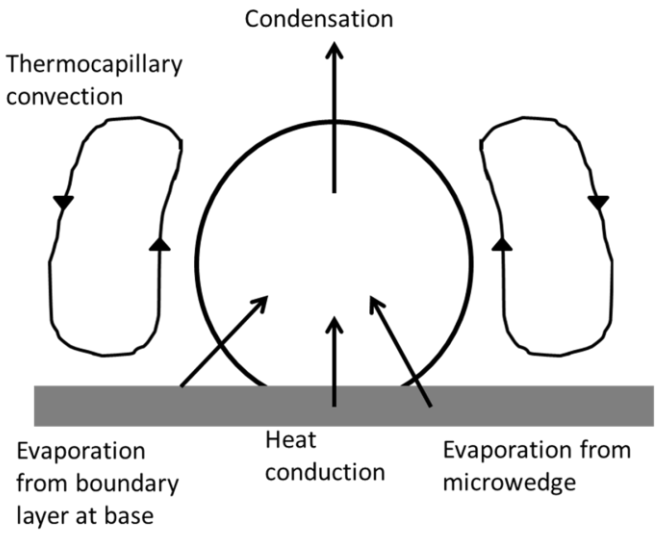

Figure 1-1. Heat flow mechanisms in boiling, after Straub [3].

surface during bubble growth. This conclusion is based on observation of nearly identical heat transfer coefficients for saturated, subcooled, microgravity, and terrestrial boiling conditions. Secondary mechanisms that contribute to boiling heat transfer are buoyancy and self-induced dynamics of bubbles.

To allow for practical application of boiling, several correlations have been developed based of various system parameters, the most widely used of which was developed by Rohsenow [4,5]. However, these correlations are unable to incorporate many of the fundamental mechanisms seen during boiling such as jet flows and the application or absence of external forces. Despite decades of study to determine a mechanistic prediction of boiling rather than simply correlations, there are no comprehensive models because of the complexity of the subprocesses involved in boiling. Dhir [6] summarizes these subprocesses to be the following: heat transfer mechanisms such as transient conduction, evaporation at bubble base, evaporation at bubble boundary, thermocapillary convection, and convection induced by bubble motion; bubble dynamics such as growth, merger, and departure; active nucleation site density; and the thermal response of the heater. These subprocesses are shown graphically in Figure 1-2. Straub further details the complex phenomena that exist in boiling such as nonlinearity, transitions to turbulence, three-dimensionality of single phase convective transfer, time-varying behavior, nucleation and growth, bubble interface interactions on the heater surface, large non-equilibrium effects, and interactions between the solid surface of the heater and the fluid phases existent in a two-phase system [1]. To deal with these complexities, Dhir proposes the complete numerical simulation of boiling to predict heat transfer behavior in multiple circumstances and the use of specific experiments to validate these numerical models [6]. He has found success in modeling the nucleation, growth, coalescence and departure of a single bubble [7], two bubbles [8], and three bubbles [9,10] as well as film boiling modeling [11,12]. However, he admits that application of numerical models

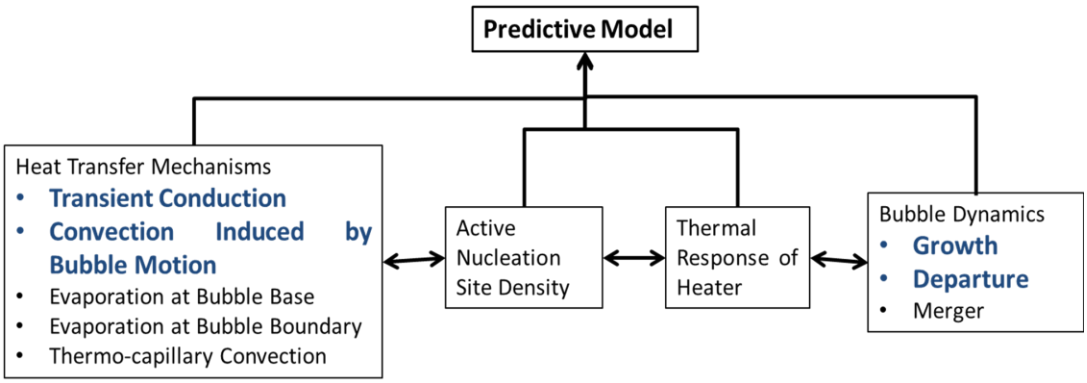

Figure 1-2. Mechanisms of boiling, after Dhir [6].

on a large scale will require additional future advances in technology and validation from results of experiments to investigate the various boiling mechanisms.

Shekriladze has also reviewed the basic mechanisms of heat transfer in boiling [13], but provides a different view on boiling mechanisms as he seeks to clear up two incorrect assumptions. The incorrect assumption is to connect the heat transfer coefficient to cooling mechanisms, and Shekriladze refers to this as the model of "the theatre of actors." Rather he advocates the use of a method of "the theatre of director" where the nucleation site is the main parameter of interest and additional factors can be incorporated in a multifactoring concept. The second incorrect assumption is the claim that microlayer evaporation comprises the majority of heat transfer during boiling. He claims that the pumping effect of growing bubble (PEGB) allows not only for heat to be transferred through phase change, but that liquid flow in the region of the growing bubble can be pumped away from the heater, resulting in high heat transfer rates. These liquid flows speed up around the bubble and have accelerations of two orders of magnitude above gravitational acceleration. This mechanism then dwarfs the contributions of Marangoni convection, microlayer evaporation, and bubbling or bubble departure. These types of contradictions are seen in much of the boiling literature.

Di Marco has studied the effects of applied electric fields to boiling, both in microgravity and in terrestrial gravity [14] with the intent of applying his results to thermal management systems in

space. His results have shown that microgravity experiments have a lower onset heat flux (which is the lowest heat flux for boiling to occur) but that the application of the electric field with a power consumption of about 50 mW is able to reduce the temperature overshoot or superheat at onset. In another experiment, results showed that force fields, such as gravity or electric fields, have minimal effect on the heat transfer coefficient, but that they greatly affect the vapor characteristics of the bubble. Larger vapor bubbles are seen in microgravity, but application of an electric field can restore these bubbles to similar sizes of those seen during terrestrial experiments with no electric field. Additionally, Di Marco observed that the critical heat flux (the maximum heat flux that the system can experience before failure occurs) is lower in microgravity, but can be enhanced by the application of an electric field, in both microgravity and terrestrial conditions. He concludes that nucleate boiling could be used in thermal management systems in space, especially because electrical fields are able to compensate in some ways for the lack of buoyancy forces, but that there is a need for additional research for practical applications of boiling.

1.2. Overview of Thesis

This thesis is prepared in a multi-paper format, in accordance with the requirements of the Graduate School of Utah State University. Chapter 2 provides a review of the literature concerning boiling onset, heat flux effects on steady state heat transfer, surface geometry effects on heat transfer, and jet flow behavior. Chapters 3 and 4 are each comprised of papers that have been submitted and are pending review to the International Journal of Heat and Mass Transfer and the Journal of Heat Transfer, respectively. Finally, Chapter 5 presents the major conclusions based on the research.

1.3. Research Objectives

The principal objective of this work is to increase understanding of boiling behavior in microgravity. This overall goal may be broken down into smaller objectives as follows:

- Record images of boiling behavior in microgravity and terrestrial gravity.
- Develop a two-dimensional, transient heat conduction model to explain wire twisting effects on bubble growth, superheating temperature, and onset conditions.
- Confirm results from conduction model with observed behavior during microgravity experiment.
- Develop analysis methods to approximate the contribution of jet flows to heat transfer and characterize jet flow behavior.

1.4. References

[1] Straub, J., 2001, "Boiling Heat Transfer and Bubble Dynamics in Microgravity," Advances in Heat Transfer, Hartnett, J., Irvine, T., Cho, Y., Greene, G. eds., Elsevier, London, **35**, pp. 57-172.

[2] Koeln, J.P, Boulware, J.C., Ban, H., and Dennsion, J.R., 2011, "Observations on Braided Thin Wire Nucleate Boiling in Microgravity," Intl. J. of Heat and Fluid Flow, **32**(5), pp. 973-981.

[3] Marek, R., and Straub, J., 2001, "The Origin of Thermocapillary Convection in Subcooled Nucleate Pool Boiling," Intl. J. of Heat Transfer, **44**(3), pp. 619-632.

[4] Incropera, F.P., Dewitt, D.P., Bergman, T.L., Lavine, A.S., 2007, Fundamentals of Heat and Mass Transfer, sixth ed., John Wiley & Sons, Hoboken, NJ, pp. 433-434,625-631, Chap. 7&10.

[5] Rohsenow, W.M., 1952, "A Method of Correlating Heat-Transfer Data for Surface Boiling Liquids," Trans. ASME, **74**(6), pp. 969-975.

[6] Dhir, V.K., 2006, "Mechanistic Prediction of Nucleate Boiling Heat Transfer – Achievable or a Hopeless Task?," J. of Heat Transfer, **128**(1), pp. 1-12.

[7] Dhir, V.K., 2001, "Numerical Simulations of Pool-Boiling Heat Transfer," AlChE J., **47**(4), pp. 813-834.

[8] Dhir, V.K., Abarajith, H.S., and Li, D., 2007, "Bubble Dynamics and Heat Transfer during Pool and Flow Boiling," Heat Transfer Eng., **28**(7), pp. 608-624.

[9] Son, G., and Dhir, V.K., 2007, "A Level Set Method for Analysis of Film Boiling on an Immersed Solid Surface," Numerical Heat Transfer, Part B: Fundamentals: An Intl. J. of Computation and Methodol., **52**(2), pp. 153-177.

[10] Son, G., and Dhir, V.K., 2008, "Three-dimensional Simulation of Saturated Film Boiling on a Horizontal Cylinder," Intl. J. of Heat and Mass Transfer, **51**(5-6), pp. 1156-1167.

[11] Son, G., and Dhir, V.K., 2008, "Numerical Simulation of Nucleate Boiling on a Horizontal Surface at High Heat Fluxes," Intl. J. of Heat and Mass Transfer, **51**(9-10), pp. 2566-2582.

[12] Abarajith, H.S., Dhir, V.K., Warrier, G., and Son, G., 2004, "Numerical Simulation and Experimental Validation of the Dynamics of Multiple Bubble Merger During Pool Boiling Under Microgravity Conditions," Annals of the New York Academy of Sciences, **1027**, pp. 235-258.

[13] Shekriladze, I.G., 2008, "Boiling Heat Transfer: Mechanisms, Correlations and the Lines of Further Research," The Open Mechanical Engineering J., **2**, pp. 104-127.

[14] Di Marco, P., and Grassi, W., 2002, "Motivation and Results of a Long-term Research on Pool Boiling Heat Transfer in Low Gravity," Intl. J. of Thermal Sciences, **41**(7), pp. 567-585.

CHAPTER 2

LITERATURE REVIEW

2.1. Onset of Nucleate Boiling (ONB)

The transition from natural convection in 1g, or conduction in 0g, to nucleate boiling, or ONB, is often studied to demonstrate the benefits of operating in the nucleate boiling regime. The dominance of conductive heat transfer in microgravity environments results in high surface temperatures according to Fourier's law, until ONB is reached. It is therefore desirable for a microgravity thermal management system to operate in the nucleate boiling regime. The relationships among working fluid, heat flux, surface geometry, gravity, and onset temperature are studied to predict when this transition will occur for various combinations of these parameters and what type of heat transfer conditions will exist.

Straub [1] studied the heat transfer efficiencies associated with various heat flux densities while boiling subcooled degassed R113 with a 0.2 mm diameter platinum wire aboard the TEXUS 3b sounding rocket. Under the lowest heat flux (17 kW/m^2), the 0g experiment boiled after reaching an onset temperature of $\Delta T_{sat,\,wire} = T_{wire} - T_{sat}$ = 34 K and then dropped to $\Delta T_{sat,\,wire}$ = 18 K after boiling was initiated. For the 1g experiment under the same heat flux, natural, buoyancy-based convection adequately cooled the wire, preventing the transition to nucleate boiling. At the median heat flux density (39 kW/m^2), the 0g experiment continued to boil with a 4 K wire temperature increase from the previous heat flux level, resulting in a final $\Delta T_{sat,\,wire}$ = 22 K after the wire superheated. The 1g experiment at 39 kW/m^2 still did not boil, but the $\Delta T_{sat,\,wire}$ increased to 30 K, a 20 K increase from the previous level. The final heat flux density (77 kW/m^2) produced boiling in both the 0g and 1g experiments. The 0g experiment, however,

showed a 6% increase in the heat transfer coefficient when compared with the 1g experiment. This experiment showed that at certain heat flux densities, 0g heat transfer can be more effective than the 1g equivalent; however, it never addressed whether this apparent increase was within the uncertainty of the system.

Zell et al. [2] also performed an experiment on the TEXUS 5 sounding rocket. This experiment also boiled subcooled degassed R113 with a 0.2 mm diameter platinum wire. The onset superheated temperatures of the wires ($\Delta T_{sat,\ wire}$) varied heavily with gravity. The 0g onset temperature was 25% more than the 1g equivalent. This onset temperature difference was conjectured to be due to the fact that the fluid in proximity to the wire in the 0g experiment was quite transient in its temperature prior to the ONB. The 1g experiment, however, had reached a steady state wire temperature because of the effects of natural convection well before boiling.

Wan and Zhao [3] used a temperature controlled pool boiling device to boil subcooled, degassed R113 with a 60 μm diameter platinum wire. The ONB was determined by the onset of explosive boiling, which occurred as soon as the heater temperature (T_{wire}) was increased to a higher set-point. This temperature set-point was the same for 1g and 0g, leading Wan and Zhao to conclude that the onset of boiling temperature is weakly dependent, or independent, of gravity.

These previous studies (except for that by Wan and Zhao) show that the ONB in microgravity is distinctly different than ONB in 1g and often results in an enhancement to the heat transfer; however, they fail to specify the conditions and system parameters that determine the ONB. The current experiment aims to study the effects of wire geometry and power input on the ONB by observing: (i) the heat flux required to transition from natural convection to nucleate boiling in 0g and 1g; (ii) the decrease in average wire temperature (T_{wire}) after the transition into boiling; and (iii) its associated explosion of bubbles along the heating element.

Additionally, the maximum superheated temperature necessary to trigger boiling incipience at the surface is an important factor in the ONB determination. For homogenous nucleation, this

value is $0.9T_c$, which is 90% of the critical temperature of the fluid [4,5]. The superheat temperature for heterogeneous nucleation is lower than that of homogenous nucleation [6]. However, no consideration is made for surface geometry effects nor the explosive growth and departure of bubbles when boiling is initiated.

2.2. Heat Flux Effect on Steady State Heat Transfer

Once the threshold heat flux input is provided to initiate boiling, the effectiveness of heat transfer can vary with the magnitude of the input heat flux and surface geometry, and is quantified in the heat transfer coefficient, h, given by Newton's law of cooling.

As stated before, Straub [1] discovered that under a given heat flux, where both 0g and 1g experiments boiled, the 0g wire temperature (T_{wire}) was actually lower than that of the 1g condition. This led Straub to conclude that the 0g steady state boiling was 6% more effective than 1g boiling. This is highly unexpected since the 0g experiment is missing the seemingly major driving force of buoyancy.

In another experiment by Straub [7,8], the enhancement of heat transfer in 0g appears to be a function of heat flux and wire diameter. In this experiment, two platinum wires of 0.05 and 0.2 mm were used to boil saturated R134a. The 0.2 mm wire showed heat transfer enhancements of up to 10% for lower power levels, but the enhancement decreased with increasing heat flux. The 0.05 mm wire showed a nearly constant enhancement of about 10% and eventually burned out. Straub's [7] results also showed that 0g boiling is either slightly enhanced or the same as a 1g experiment for a given wire superheat temperature ($\Delta T_{sat,\ wire}$), but the effectiveness did not seem to relate to power input.

Although Straub studied the effect of wire diameter and gravity level on steady state heat transfers with a set heat flux, there is still a need to confirm these results across different

operating conditions. The current experiment seeks to resolve these issues by studying the effects of heat flux on the steady state heat transfer effectiveness by observing the heat transfer coefficient for various heat fluxes and surface geometries during steady state boiling of subcooled water.

2.3. Surface Geometry Effects on Heat Transfer

The surface characteristics of the heating element affect bubble generation and departure dynamics, which, in turn, affect the heat transfer coefficient. As previously mentioned, Straub [7] showed that a smaller diameter wire was constantly more effective at dissipating heat in 0g than in 1g, but a larger diameter wire was less able to withstand higher heat fluxes without wire burnout. Further Straub [1] justifies the use of a thin platinum wire as a heating surface because of the advantage of using the wire as a heater and a resistance thermometer, the well-defined temperature characteristics, and the ability of the wire to deal with high temperatures.

Boiling heat transfer is a strong function of the surface geometry of the heater. Straub's experiment [1] showed that 0g boiling was up to 15% more effective in microgravity when the heat transfer coefficients of each gravity level were compared. In later wire boiling experiments [7,8], he concluded that heat transfer enhancement in 0g is a function of heat flux and wire diameter. Recent studies on nano-particle deposition on the surface [9] were found to have an increase in the heat transfer coefficient. Porous materials such as open celled metallic foam [10] and a multi-scaled modulated porous structure [11] were also shown to enhance boiling heat transfer.

Fukada et al. [12] studied the effects of calcium carbonate fouling on platinum wires of various diameters ranging from 0.01 mm to 0.2 mm. Saturated water was boiled in both 0g and 1g with both bare wires and wires with a coating of calcium carbonate. The scaling on the wires

created large, discrete nucleation sites, which prevented the coalescence of bubbles widely seen on the single smooth wire. The bubble departure diameters from the scaled wire were also relatively smaller. The bubble coalescence on the bare wires eventually led to the development of large engulfing bubbles, which resulted in burnout. Therefore, critical heat flux (CHF) was effectively increased because of the scale on the wires preventing bubble coalescence.

Chyu and Mghamis [13] investigated the heat transfer enhancement achieved by connecting two hollow, stainless steel tubes in line contact. They determined that the restricted region between the tubes had low wall superheats and provided a restricted geometry that was favorable to vapor bubble formation. Because of the operation of this experiment in a terrestrial laboratory, buoyancy effects prevented the heat transfer enhancement from existing anywhere except on the upward face of the twisted tubes. A microgravity environment could allow that enhancement to be experienced by the entire wire surface.

Past research has concluded that surface geometry plays a role in boiling dynamics but has not answered the questions about specific surface characteristic effects on microgravity boiling. The current experiment seeks to fill that gap by testing the effect of two unique wire geometries, a three-wire and a four-wire twist.

2.4. Jet Flows Existent in Subcooled Nucleate Boiling

Although boiling has been studied extensively, the last 10 years have shown an increase in the literature concerning jet flow behavior. Technological advances in optical measurements as well as the use of microgravity environments have allowed researchers to investigate the behavior of this phenomenon. These jet flows are of particular interest because of the role these jets flows have in achieving the high heat fluxes observed in nucleate boiling [14].

Jet flows are a separate, observed mode of boiling heat transfer, compared to standard bubble nucleation, growth, and departure. Wang et al. [15] characterize several different modes of jets (high-energy liquid jet, fog-like jet, cluster-like jet, bubble-forming jet, bubble-bunch jet, and bubble-top jet) that are produced depending on the fluid, level of subcooling, and applied heat flux. Using these initial observations, his research group continued to study these jet flows and characterized additional modes of jet flows in subcooled nucleate boiling, such as the multi-jet [16,17], large bubble, small explosive bubbles, and coexisting bubble boiling [18]; further, the group characterized their enhancement on heat transfer [19]. After characterization of these modes, the heat transfer performance of the coexisting bubble boiling was approximated as a sum of the large and small explosive bubble modes of boiling, based on their equilibrium currents. The current project confirms this same coexistent behavior. Additionally, a relative bubble area comparison is used to approximate the heat flux distribution of a proposed new mode of boiling jet flow. Additionally, the influence of microgravity on these boiling modes is investigated, because of the ability to notice unique behavior [14].

The development and characteristics of these jet flows are greatly influenced by thermocapillary forces (Marangoni forces), which exist in subcooled boiling [20-22], although Straub observes that these forces participate more as a transport mechanism than a heat transfer mechanism [23]. Conversely, Shekriladze concludes that jet flows can have a pumping effect, which explains the high heat transfer rates observed and that the jet flow is generated due to non-uniformity of evaporation of the bubble when its growth remains in the layer with a high temperature gradient [24-26]. Lu investigated the development of bubble jet flows and characterizes them into three stages of waiting, burst, and stably developing stage, and he observed that the bubble jet flows exist on bubbles of radius 0.01-0.30 mm and extend into the fluid a distance of 0.5-2.0 mm [27].

2.5. Summary

After reviewing the literature, there is an obvious need to further resolve which mechanisms are the major contributors to heat transfer and to better understand their behavior. Additionally, there is a need for analysis methods for boiling video to provide quantitative means of relating heat transfer to the observed bubble dynamics. Other researchers have shown that modifying the surface geometry can provide heat transfer enhancements. It is important to further investigate the form that these enhancements can take such as heat transfer coefficient improvements, reduction of magnitude and duration of wire superheating, and reduction of boiling onset to quickly transition from conduction to boiling dominated heat transfer. This final consideration is particularly important in microgravity where natural convection is absent. Finally, there is a need to investigate boiling behavior of jet flows and characterize additional modes of jet flows that are observed.

2.6. References

[1] Straub, J., 2006, "Highs and Lows of 30 Years Research of Fluid Physics in Microgravity, a Personal Memory," Microgravity Sci. and Technol., **18**(3-4), pp. 14-20.

[2] Zell, M., Straub, J., and Weinzieri, A., 1984, "Nucleate Pool Boiling in Subcooled Liquid under Microgravity—Results of TEXUS Experimental Investigations," Proceedings of the 5th European Symposium on Material Sciences under Microgravity, Schloss Elmau.

[3] Wan, S.X., and Zhao, J.F., 2008, "Pool Boiling in Microgravity: Recent Results and Perspectives for the Project DEPA-SJ10," Microgravity Sci. and Technol., **20**(3-4), pp. 219-224.

[4] Xu, J., and Zhang, W., 2008, "Effect of Pulse Heating Parameters on the Microscale Bubble Dynamics at a Microheater Surface," Intl. J. of Heat and Mass Transfer, **51**(1-2), pp. 389–396.

[5] Delhaye, J.M., and McLaughlin, J.B., 2003, "Appendix 4: Report of Study Group on Microphysics," Intl. J. of Multiphase Flow, **29**(7), pp. 1101-1116.

[6] Quan, X., Chen, G., and Cheng, P., 2011, "A Thermodynamic Analysis for Heterogeneous Boiling Nucleation on a Superheated Wall," Intl. J. of Heat and Mass Transfer, **54**(21-22), pp. 4762-4769.

[7] Straub, J., 2005, "Bubble – Bubbles – Boiling," Microgravity Sci. and Technol., **16**(1), pp. 242-248.

[8] Straub, J., Zell, M., and Vogel, B., 1993, "What We Learn From Boiling under Microgravity," Microgravity Sci. and Technol., **6**(4), pp. 239-247.

[9] Huang, C.K., Lee, C.W., and Wang, C.K., 2011, "Boiling Enhancement by TiO_2 Nanoparticle Deposition," Intl. J. of Heat and Mass Transfer, **54**(23-24), pp. 4895-4903.

[10] Xu, Z.G., Qu, Z.G., Zhao, C.Y., and Tao, W.Q., 2011, "Pool Boiling Heat Transfer on Open-celled Metallic Foam Sintered Surface under Saturation Condition," Intl. J. of Heat and Mass Transfer, **54**(17-18), pp. 3856-3867.

[11] Li, C.H., Li, T., Hodgins, P., Hunter, C.N., Voevodin, A.A., Jones, J.G., and Peterson, G.P., 2011, "Comparison Study of Liquid Replenishing Impacts on Critical Heat Flux and Heat Transfer Coefficient of Nucleate Pool Boiling on Multiscale Modulated Porous Structures," Intl. J. of Heat and Mass Transfer, **54**(15-16), pp. 3146-3155.

[12] Fukada, Y., Haze, I., and Osakabe, M., 2004, "The Effect of Fouling on Nucleate Pool Boiling of Small Wires," Heat Transfer-Asian Res., **33**(5), pp. 313-329.

[13] Chyu, M.C., and Mghamis, A.M., 1991, "Nucleate Boiling on Two Cylinders in Line Contact," Intl. J. of Heat and Mass Transfer, **34**(7), pp. 1783-1790.

[14] Peng, X.F., Wang, Z., and Lee, D.J., 2004, "Dynamic Behavior of Vapor Interface during Nucleate Boiling," J. Chin. Inst. Chem. Engrs., **35**(4), pp. 467-475.

[15] Wang, H., Peng, X.F., Wang, B.X., and Lee, D.J., 2002, "Jet Flow Phenomena During Nucleate Boiling," Intl. J. of Heat and Mass Transfer, **45**(6), pp. 1359-1363.

[16] Shekriladze, I.G., 2006, "Discussion: 'Dynamics of Bubble Motion and Bubble Top Jet Flows from Moving Vapor Bubbles on Microwires' (Christopher, D.M., Wang, H., and Peng, X., 2005, Journal of Heat Transfer, **127**, pp. 1260-1268)," J. of Heat Transfer, **128**(12), pp. 1343-1344.

[17] Christopher, D.M., Wang, H., Peng, X., and Garimella, S.V., 2006, "Closure to 'Discussion: "Dynamics of Bubble Motion and Bubble Top Jet Flows from Moving Vapor Bubbles on Microwires" (Christopher, D.M., Wang, H., and Peng, X., 2005, Journal of Heat Transfer, 127, pp. 1260-1268)'," J. of Heat Transfer, **128**(12), pp. 1345-1346.

[18] Lu, J.F., Peng, X.F., and Bourouga, B., 2006, "Nucleate Boiling Modes of Subcooled Water on Fine Wires Submerged in a Pool," Exper. Heat Transfer, **19**(2), pp. 95-111.

[19] Wang, H., Peng, X.F., Wang, B.X., and Lee, D.J., 2003, "Bubble Sweeping and Jet Flows During Nucleate Boiling of Subcooled Liquids," Intl. J. of Heat and Mass Transfer, **46**(5), pp. 863-869.

[20] Henry, C.D., Kim, J., and McQuillen, J., 2006, "Dissolved Gas Effects on Thermocapillary Convection During Boiling in Reduced Gravity Environments," Heat and Mass Transfer, **42**(10), pp. 919-928.

[21] Petrovic, S., Robinson, T., and Judd, R.L., 2004, "Marangoni Heat Transfer in Subcooled Nucleate Pool Boiling," Intl. J. of Heat and Mass Transfer, **47**(23), pp. 5115-5128.

[22] Zhukov, S.A., Afanas'ev, S.Y., and Echmaev, S.B., 2003, "Concerning the Magnitude of the Maximum Heat Flux and the Mechanisms of Superintensive Bubble Boiling," Intl. J. of Heat and Mass Transfer, **46**(18), pp. 3411-3427.

[23] Straub, J., 2002, "Origin and Effect of Thermocapillary Convection in Subcooled Boiling: Observations and Conclusions from Experiments Performed at Microgravity," Annals of the New York Academy of Sciences, **974**, pp. 348-363.

[24] Shekriladze, I.G., 2003, "Comment on the paper by H. Wang, X.F. Peng, B.X. Wang, and D.J. Lee 'Jet flow phenomena during nucleate boiling' IJHMT 45 (6) (2002) 1359-1363," Intl. J. of Heat and Mass Transfer, **46**(14), pp. 2711-2712.

[25] Shekriladze, I.G., 1966, "On the Mechanism of Nucleate Boiling," Bull. Academy of Science Georgian SSR, **41**(2), pp. 392-396 (English version: Technical Report NASA TM X-59398, 1967, pp. 1-10).

[26] Shekriladze, I.G., 1970, "On the Role of the 'Pumping Effect' of a Vapor Bubble Growing at the Wall During Nucleate Boiling," Problems of Convective Heat Transfer and Steam Purity, V.G. Ratiani, ed., Metsniereba Press, Tbilisi, pp. 90-97.

[27] Lu, J.F., and Peng, X.F., 2007, "Bubble Jet Flow Formation during Boiling of Subcooled Water on Fine Wires," Intl. J. of Heat and Mass Transfer, **50**(19-20), pp. 3966-3976.

CHAPTER 3

SURFACE GEOMTERY EFFECT ON BUBBLE ONSET IN MICROGRAVITY POOL BOILING

This chapter is a paper[a] submitted as a journal article in the International Journal of Heat and Mass Transfer, pending review. All permissions for using this paper as a part of this thesis are contained in Appendix A.

3.1. Abstract

Nucleate boiling is an effective method of transferring heat, yet its application in microgravity requires greater understanding for practical use in thermal management systems. To further this knowledge base, a microgravity boiling experiment was performed (floating) onboard an aircraft flying in a parabolic trajectory to study the effects of surface geometry and heat flux on subcooled, pool boiling of water. With three different wire geometries and five different heat flux levels, heat transfer behavior at onset and steady state boiling was recorded and analyzed. A special emphasis was the investigation of heat transfer enhancement caused by modifying the surface geometry through the use of a twist of three wires and a twist of four wires. A new method for bubble analysis was developed to quantify bubble growth characteristics, which allows a quantitative comparison of bubble dynamics between different data sets. It was found that the surface geometry of the three-wire twist enhanced heat transfer by reducing the boiling onset heat flux and the average wire temperature in microgravity. Addition of more wires in the twist reduced this enhancement as the behavior further approaches the behavior of a single wire.

[a] Coauthors: Justin P. Koeln, Andrew W. Fassmann, Robert J. Barnett, and Heng Ban

Simulation results indicated that increased local superheating in wire crevices may be responsible for the change of boiling behavior. The boiling heat transfer rate, in comparison to ground experiments, was lower for microgravity at low heating rates, and higher at high heating rates, regardless of the wire geometry. The result of this study could lead to new designs of surface geometry for microgravity applications.

3.2. Introduction

Nucleate boiling has been extensively studied because of its high heat transfer rates and wide applications in energy production and thermal management systems. However, its fundamental behavior in microgravity is not well understood because of the complex interactions of surface and other forces, excluding buoyancy, in the two-phase heat transfer. Furthermore, there is a lack of analytical techniques in the literature to provide a quantitative measurement of bubbles in boiling video data.

Several excellent reviews have summarized research on the topic of boiling in microgravity [1-3]. One of the early microgravity experiments was Straub's sounding rocket experiment [4], which reported that the 0-g boiling onset temperature was 25% greater than its 1-g equivalent. Straub concluded that this difference is from the highly transient temperature of the fluid in proximity to the wire in microgravity, while the 1-g case was able to reach a steady state temperature because of natural convection. This microgravity transient behavior results in distortions in the temperature field, which could be a driving force for bubble and fluid motion [5]. Conversely, Zhao's [6] more recent study using a temperature controlled pool boiling device concluded that the onset of nucleate boiling is weakly dependent or independent of gravity because boiling occurred at the same temperature set-point for both gravity levels. These somewhat conflicting results continue to occur in the literature. Prior to the onset of nucleate

boiling, Petrovic [7] concludes that there is a dominance of Marangoni convection after the natural convection regime and before nucleate boiling, when dissolved air bubbles begin to form. He suggests that this effect should not be assumed negligible for terrestrial boiling heat transfer. Straub [1] suggested that non-condensable gasses cause Marangoni convection, leading to the departure of bubbles. Wan [8] and Kannengieser et. al [9] further proposed that these gasses are not the only cause of Marangoni convection. Rather, the driving force is from evaporation near the heater surface and condensation near the top of the bubble. These progressive and sometimes conflicting results and theories clearly show that more study must be done to fully understand nucleate boiling phenomena in microgravity.

Boiling heat transfer is a strong function of the surface geometry of the heater. Straub's experiment [10] showed that 0-g boiling was up to 15% more effective in microgravity when the heat transfer coefficients of each gravity level were compared. In later wire boiling experiments [11,12], he concluded that heat transfer enhancement in 0-g is a function of heat flux and wire diameter. Recent studies on nano-particle deposition on the surface [13] were found to have an increase in the heat transfer coefficient. Porous materials such as open celled metallic foam [14] and a multi-scaled modulated porous structure [15] were also shown to enhance boiling heat transfer. Fukada [16] investigated the behavior of surface enhancements in microgravity. One experiment studied the effects of a micropinned surface and the other focused on how calcium carbonate fouling affects heat transfer on thin wire, saturated boiling in microgravity. The fouled wire exhibited a smaller bubble departure diameter because the calcium carbonate scales inhibited bubble coalescence, resulting in an increased critical heat flux. The clean, smooth wire in the experiment generated a large insulating bubble that caused the wire to burnout. Chyu and Mghamis [17] further studied the effect of surface geometry on boiling heat transfer by twisting two hollow tubes together in terrestrial gravity. The twist of the tubes created a restricted or creviced region that caused a local high temperature region and hence initiated boiling when the

tubes were heated. However, this enhancement was affected by wire orientation because of buoyancy effects.

The objective of the current study is to explore the effect of surface geometry, through wire twisting and heat flux variations on nucleate pool boiling in microgravity. The terrestrial and microgravity experiments used a constant-current heated wire with temperature measurement and visual recordings to study the effect of various heat fluxes and surface geometries on heat transfer behavior and bubble dynamics. A new method was also developed to quantify visual measurements of vapor formation.

3.3. Experimental Setup

A test rig capable of supplying power, taking measurements, and storing additional experimental fluid chambers was built to operate on a modified Boeing 727 for the parabolic flight. A total of 20 parabolas were flown with each providing about 20 s of microgravity. To provide similar initial conditions for each microgravity parabola, fifteen fluid chambers were tested according to the parameters shown in Table 4-1. One of the issues with determining the average heat flux of each wire geometry is that the heat flux is not axisymmetric for the twisted wire geometries because of localized heating in the crevices. To take this into consideration, the heat flux for the three-wire geometry was calculated based on the external surface area of the three-wire twist, which is taken as 5/6 of the entire surface area of three separate cylinders, to exclude the area in the crevice. Similarly, the four-wire geometry was treated as four separate cylinders and then multiplied by 3/4. One third of the chambers contained a single 130 μm diameter platinum wire, another third contained three 76 μm diameter platinum wires that were twisted together, and the final third contained four 51 μm diameter platinum wires also twisted together. These wire configurations, represented in Figure 3-1a, produce cross sections with

Table 4-1. Experimental conditions performed (* indicates lowest heat flux where boiling was observed)

Geometry (Experimental condition)	Average Power (W)	Heat Flux (kW/m^2)	Steady state wire temperature (°C) in microgravity
Single Wire (1)	2.48	600	N/A
Single Wire (2)	3.11	750*	86.9
Single Wire (3)	3.36	790	94.6
Single Wire (4)	4.40	1030	92.1
Single Wire (5)	4.93	1170	95.1
Three-Wire (1)	2.35	400	N/A
Three-Wire (2)	3.17	500*	87.4
Three-Wire (3)	3.32	560	91.5
Three-Wire (4)	4.41	670	88.7
Three-Wire (5)	4.48	780	91.4
Four-Wire (1)	2.47	510*	80.5
Four-Wire (2)	3.04	640	87.9
Four-Wire (3)	3.66	760	90.3
Four-Wire (4)	4.44	930	90.4
Four-Wire (5)	4.70	990	89.4

similar areas and comparable resistances (±8%). The ends of each 1 cm long wire were pinched in an electrical terminal which was located at the end of stainless steel rods to provide electrical power and structural support. Beneath the platinum wire heater is a ladder of four Type T thermocouples (TC 1-4) shown on the right in Figure 3-1b. This assembly is placed inside a polycarbonate fluid chamber, shown on the left of Figure 3-1b, designed to hold 164 mL of deionized, degassed, subcooled water. Polycarbonate walls and the epoxy seals allowed for flexing of the sidewalls in order to reduce the effects of internal pressure changes from vapor formation.

The test rig allowed three fluid chambers to be tested at a time inside the free floating structure. Prior to each microgravity parabola, the free float section was released to reduce the residual vibrations of the aircraft. After each microgravity parabola and during periods of hypergravity, three new chambers from the storage crate would replace the tested chambers inside

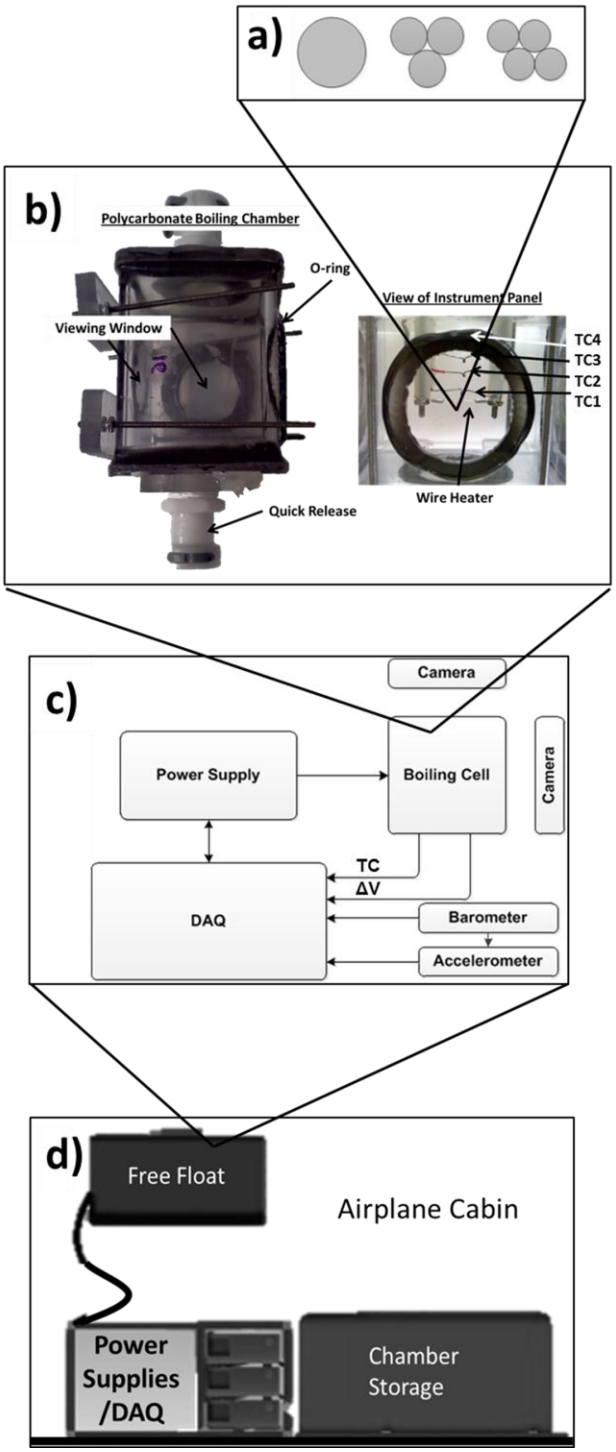

Figure 3-1. Flight equipment description: wire heater cross-sections (a), fluid chamber diagram (b), system diagram (c), and test rig diagram (d).

the free float structure. Operation of the experiment followed the schematic shown in Figure 3-1c during each microgravity parabola. The data acquisition system (DAQ) selected one of five pre-programmed, constant current levels whose average power after boiling is shown in Table 4-1, to provide power to the wire heater in each fluid chamber. The platinum wire heater was also used as an RTD to determine the average temperature of the wire. Measurements of current to the wire heater and voltage drop across the wire heater were taken at approximately 10,000 Hz with the average and standard deviation being recorded every 10 ms. Pressure and accelerometer measurements were also taken in the same manner and yielded an average ambient pressure of 82.1 kPa (±0.1kPa) and an average acceleration of 10^{-2} g (top of Figure 3-2) during each microgravity parabola due to the free float structure (Figure 3-1d). Thermocouple measurements were taken at 75 Hz. Each fluid chamber had two orthogonal video cameras recording at 30 fps and at a resolution of 1920 x 1080 pixels. Magnifying lenses provided a pixel resolution of about 14 μm x 14 μm. A diffused, red LED and a harsh white LED provided lighting for each fluid chamber.

3.4. Results and Discussion

The results of this experiment are summarized and discussed in three subsections: the observed effects of heat flux and surface geometry, the onset conditions for boiling, and the steady state characteristics once boiling is achieved. Observed onset conditions were compared to a finite volume conduction model for the wire geometries. Steady state heat transfer coefficients of terrestrial results were compared to the microgravity data to investigate heat transfer enhancement in microgravity. Finally, a new method for analyzing visual boiling data quantified the behavior of bubble dynamics across frames of video.

3.4.1. Experimental Observations

Figure 3-2 shows the wire temperature over time for the four-wire heating element at a heat flux of 510 kW/m^2, along with the measured acceleration for the fluid chamber. Spikes in acceleration are because operators were required to attach and detach the free floating structure. The behavior shown in Figure 3-2 is representative of the majority of temperature responses for various heat fluxes and wire geometry configurations. Time zero in the figure corresponds to the time when power to the wire was turned on and measurements were actively taken. Prior to the transition to boiling, the wire temperature rises and exceeds the saturation temperature, providing the superheating necessary to initiate boiling. As seen in the figure, this superheating period can reach relatively high temperatures corresponding to a low effective heat transfer coefficient and inefficiency. The highest degree of superheating was seen by the single wire under a heat flux of 790 kW/m^2, which reached 149 °C (over 50 °C above the saturation temperature). Due to a large degree of subcooling, the transition into boiling is associated with a significant drop in temperature. Video recordings showed that the transition to boiling is accompanied by a rapid formation and departure of bubbles, sending the hot water away from the wire and allowing cooler water to take its place. As a result of this process, as much as an 85 °C drop in wire temperature was seen by the four-wire twist under a heat flux of 510 kW/m^2. This explosion of bubbles activates the nucleation sites on the heating elements by the formation of vapor embryos in the nucleation cavities. Once vapor is present on the surface of the heater, the temperature of the wire appears to be a first order, step input transient response until a steady state temperature, associated with steady nucleate boiling, is reached. This steady state temperature was observed to be as much as 14 °C below the saturation temperature because only the average wire temperature was recorded. Although the active nucleation sites are likely above the saturation temperature, the majority of

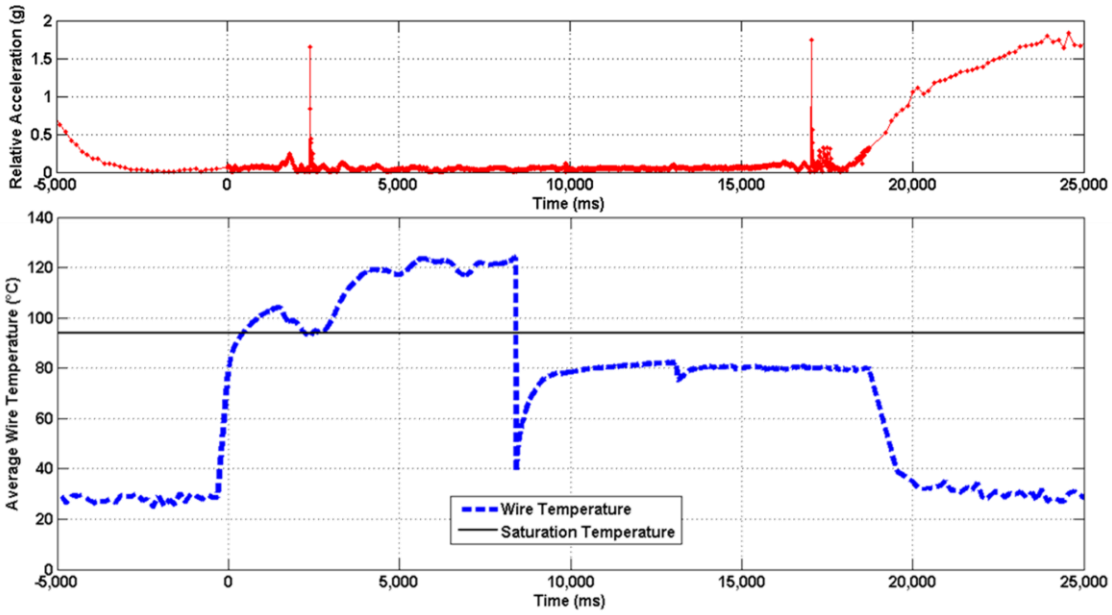

Figure 3-2. General microgravity temperature behavior and relative acceleration.

the heating element surface is cooler. The terminals holding the heating elements, while acting as large heat sinks, have a negligible effect on average wire temperature due to the high ratio (~100:1) between wire length and diameter. Radiation effects are calculated to be less than 0.1% of heat transfer (see Appendix B) and are considered negligible.

Of the various heat fluxes, only two experimental conditions resulted in data for the onset temperature for each of the three geometries. This is because the single and three-wire geometries did not boil during the first experimental condition and the majority of superheating period for the three-wire geometry at the higher heat fluxes of 670 and 780 kW/m^2 were not observed due to a 200 ms gap in the data. This gap directly following the powering of the wires was caused by a communication delay between the power supplies and data acquisition system, and it is expected that there was a superheating period for these heat fluxes that lasted less than the 200 ms. From Table 4-2, however, it can be seen that the superheating temperature for the three-wire geometry in microgravity was significantly less than that of the single and four-wire geometries for both experimental conditions. Additionally, the maximum superheated temperature achieved was 0.7

Table 4-2. Maximum wire superheat temperatures

Experimental Condition	Single wire(°C)	Three-wire (°C)	Four-wire (°C)
#2 - µg	118.9	97.5	126.4
#2 – 1g	88.8	81.5	93.5
#3 - µg	149.3	104.0	124.8
#3 – 1g	104.7	91.0	99.4

T_c of pure water, which is lower than the 0.9 T_c necessary to trigger boiling incipience of homogenous nucleation [18,19]. It is postulated that this is because the measured temperature is an average of the entire wire and the wire experiences heterogeneous nucleation [20].

3.4.2. Modeling of Onset Conditions

To understand the differences seen in boiling onset, an explicit, finite volume model was developed to calculate the evolution of the temperature profile for the three different wire geometries and five heat fluxes during the initial conductive heating phase prior to boiling. The computation domain was 400 µm x 400 µm (a 200 x 200 structured grid) and a 1 ms time step was implemented in the code to solve for the transient, two-dimensional heat equation with uniform heat generation in the wire and pure conduction in the water, Eq. (1). Constant initial temperature boundary conditions were used with the initial temperature given by thermocouple data from the actual experimental results. Modeling results show the temperature distribution in both the wire and surrounding water (water equation has no heat generation term).

$$\frac{\partial^2 T}{\partial x^2} + \frac{\partial^2 T}{\partial y^2} + \frac{q'''}{k} = \frac{1}{\alpha}\frac{\partial T}{\partial t} \tag{1}$$

In comparing the modeling results to the measured data, it became apparent that the model under-predicted the heat transfer prior to boiling, indicating that the heat transfer was not purely conductive in experiments. It is suspected that residual fluid motion from accelerations were enhancing the heat transfer and reducing the average wire temperature. Since the heating

elements are small in diameter, very little fluid motion is needed to surround the wire with fresh water at the ambient temperature, thus cooling the wire. Regardless, predicted characteristics of temperature profiles for the various heating element geometries and heat fluxes can be compared and correlated to the experimental results to better understand the effect of wire geometry.

To investigate the effect of surface geometry on boiling onset, the conduction model was run at the same power and same amount of heating time for each of the wire geometries, with the results shown in Figure 3-3. The model shows that although the wires dissipate the same power, the average temperature for the three-wire geometry can be significantly lower due to the crevices seen in Figure 3-3b. These crevices form local superheating regions, allowing the fluid to reach the superheating temperature necessary for boiling onset while reducing the average temperature of the entire wire. It is expected that these crevices enhance boiling onset because they allow the water surrounding the heating element to exceed a critical temperature, T_{cr}, nearer to the wire than if the crevice was not present. There is therefore a critical length, L_{cr}, normal to the surface of the wire(s), which accounts for the need of the liquid to exceed T_{cr} for volume distance large enough for the formation of a bubble. This effect of crevices on critical lengths can be seen in Figure 3-3d, which shows the temperature profiles along the lines given in Figure 3-3a-c. For an L_{cr} of 50 μm from the wire, the water temperature of the three-wire geometry barely decreases, while the water temperatures of the single and four-wire geometries decrease by 40 °C and 15 °C, respectively. The crevices in the three- wire geometry allow the local superheated region to extend farther into the fluid and require a lower average wire temperature for boiling incipience. For both the three- and four-wire geometries, it is expected that vapor will first form in the triangularly shaped regions in the center of the element since the water temperature in these regions exceeds that of any other region.

Furthermore, Figure 3-3a, 4–3c, and 4–3d show that the four wire geometry temperature profile is more similar to that of the single wire than the three-wire geometry. It is expected that

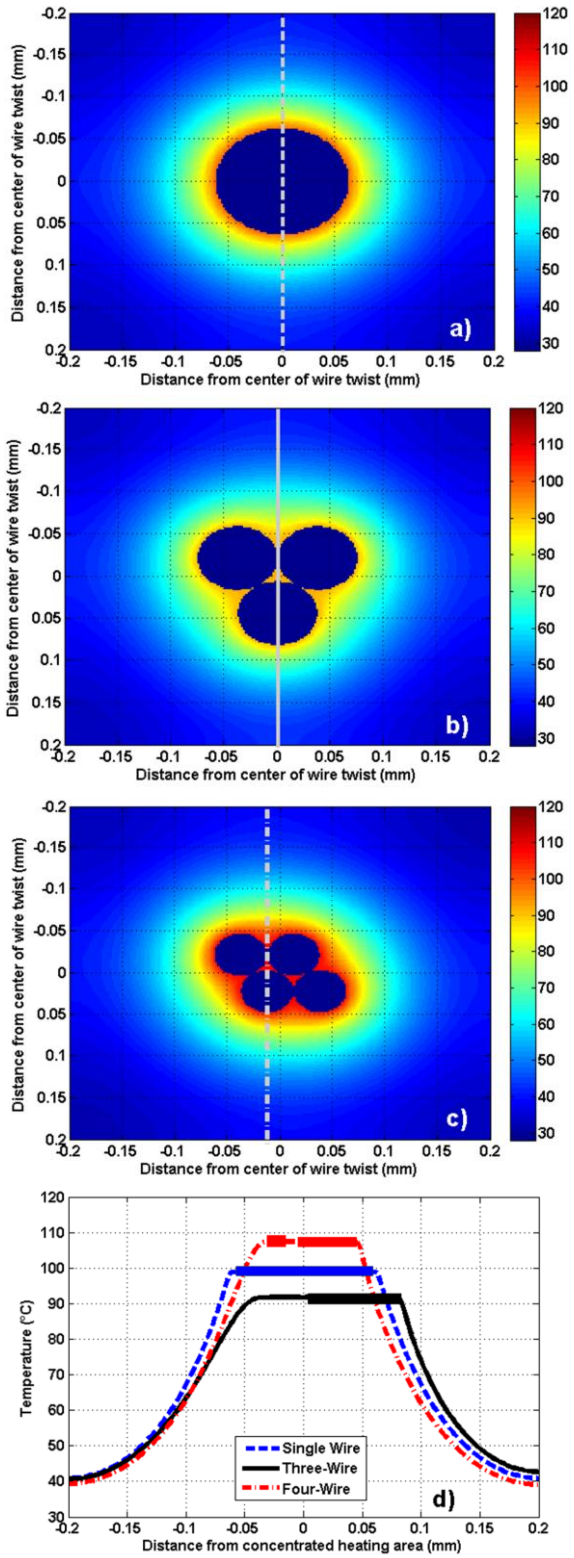

Figure 3-3. Model results after 50 ms with q=3.0 W. Single wire (a), three-wire (b), four-wire (c), temperature along contour lines with bold lines representing wire temperature (d).

as more wires are twisted to form a single heating element, the resulting heat transfer characteristics will approach that of the single wire. This could be due to the need to superheat the fluid in multiple crevices, thus distributing the heat more like a single wire and reducing local superheating temperatures near the crevices.

In addition to allowing the average wire temperature to be lower, crevices in the three- and four-wire geometries also result in a lower heat flux for boiling heat transfer to occur and a shorter length of time that the wire superheats. Figure 3-4 shows the time of superheating for all three wire geometries of the second experimental condition. The single wire geometry experiences superheating for over 1000 ms, while the three- and four-wire geometries experience 110 and 360 ms of superheating, respectively. In the case of the three-wire geometry, this short superheating time results in a lower average superheat temperature due to local superheating in the crevices, as expected. Although the four-wire geometry's period of superheating is shortened, the magnitude of its superheating is high and behaves more like the single wire geometry. To investigate this behavior, the model was run with an effective thermal conductivity for water, which was adjusted until the average wire temperature of the model matched the maximum superheat temperature of the experiment. The resulting temperature profiles at bubble onset are shown in Figure 3-5, where the single and four-wire geometry profiles look more similar to each other than to the three-wire geometry. The results indicate that bubble onset requires a certain amount of water adjacent to the wire to be above saturation temperature. In this study, it appears that water within 50 μm distance from the wire surface needs to be above saturation temperature for bubble onset. Even though the wire surface temperature for the single and four-wire geometry was above saturation before they reached the temperatures shown in Figure 3-5, bubble onset only occurred when there was enough water near the wire that was heated above the saturation temperature. This also leads to the conclusion that as more wires are added to a wire twist, the more the twist behaves like a single wire.

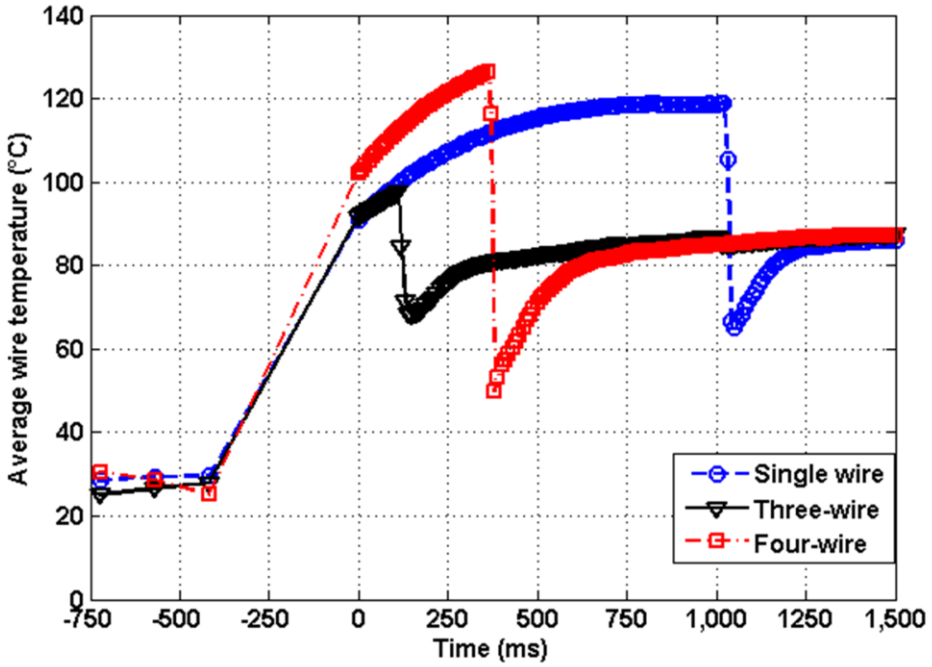

Figure 3-4. Wire temperature behavior of second experimental condition, showing superheating of different wire geometries.

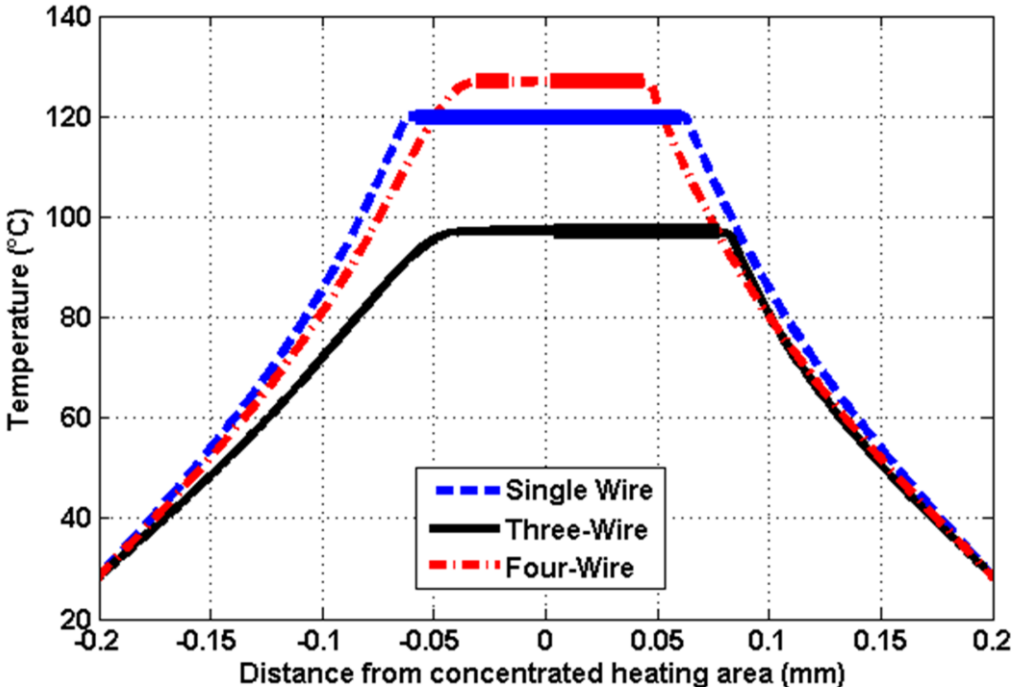

Figure 3-5. Model results using effective thermal conductivity to match experimental superheating temperatures, with bold lines representing wire temperatures.

Figure 3-6 compares the average wire temperatures of all wire geometries of the third experimental condition for both gravity levels. Comparison of the wire temperature behavior for the different geometries seen in Figure 3-4 and Figure 3-6 shows that the increase in heat flux resulted in a shortened amount of time spent superheating for all wire geometries. It is also important to note that the wire temperature behavior in microgravity has larger temperature drops compared to the ground tests at the same heat flux, and can have a lower steady-state temperature. This large temperature drop is due to the lack of natural convection to cool the wire in microgravity, and therefore, when boiling is initiated, subcooled water quickly rushes in and drops the average wire significantly.

3.4.3. Steady State Characteristics

To investigate the effect of gravity on the effectiveness of heat transfer for the system, the heat transfer coefficient for each data set was determined. This value is based on Newton's Law of cooling, Eq. (2).

$$h = \frac{q''}{(T_s - T_\infty)} \tag{2}$$

To determine the heat transfer coefficient for heat fluxes where boiling occurred, the heat transfer coefficient was averaged after boiling had been initiated and when wire temperature had reached a steady state condition. For heat fluxes where boiling did not occur or occurred much later during the test, the heat transfer coefficient was averaged over the entire period that power was supplied to the wire. Figure 3-7 shows the ratio of heat transfer coefficient in microgravity compared to normal gravity, with unity represented by the solid black line.

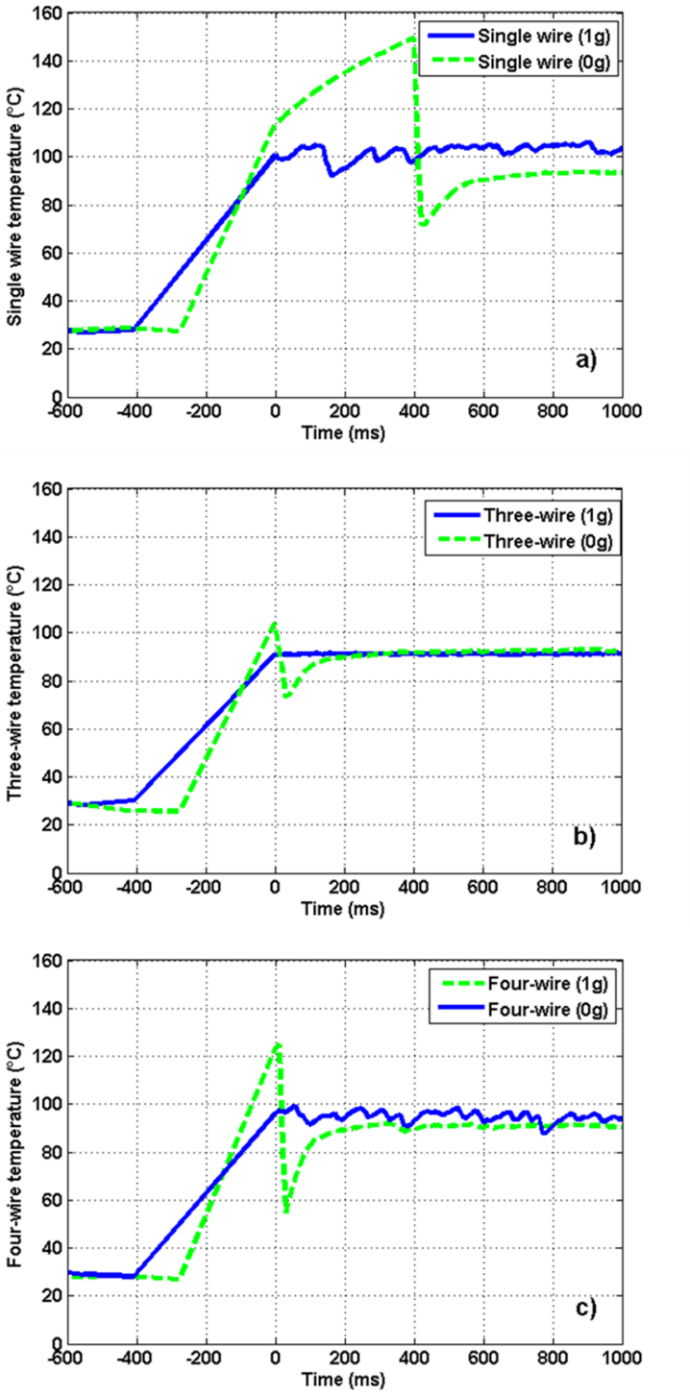

Figure 3-6. Wire temperature, geometry, gravity comparison for the third experimental condition. Single wire (a), three-wire (b), and four-wire (c).

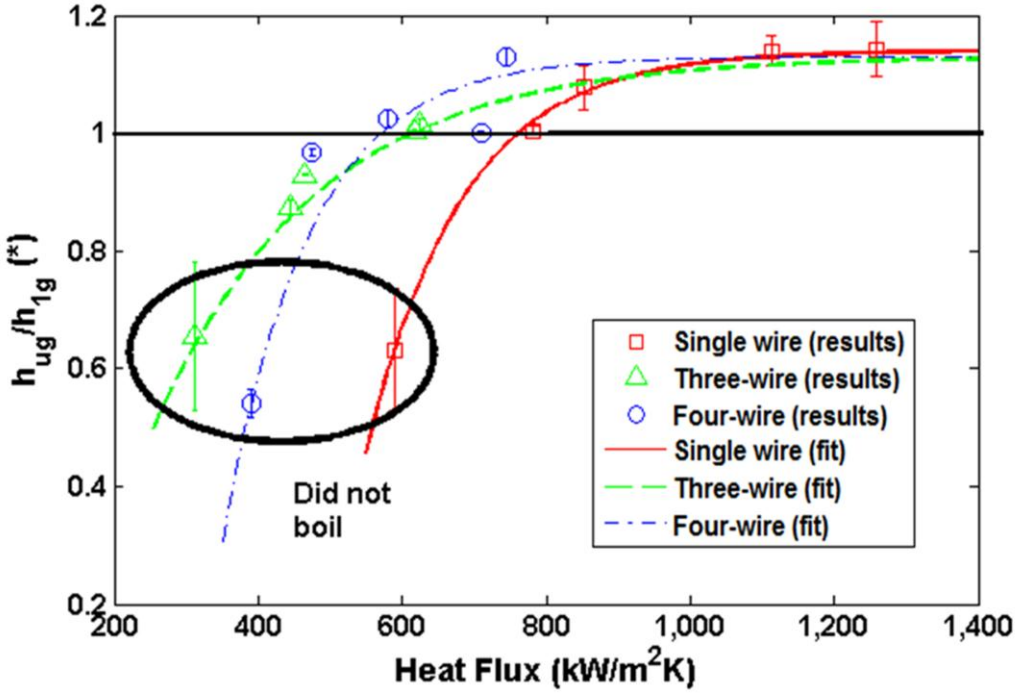

Figure 3-7. Steady state heat transfer coefficient comparison between gravity levels with uncertainty bars.

When a data point is above the line, steady state boiling heat transfer is more effective in microgravity, and when below the line, it is more effective in normal gravity. The three circled data points that are far below the line represent instances where boiling did not occur at either gravity in experiments, showing that without boiling occurring, convective heat transfer in microgravity is very inefficient. Furthermore, a Taylor Series Method uncertainty analysis [21] of the results presented in Figure 3-7 supports the conclusion that for this system, boiling heat transfer is independent of gravity and in some cases can be enhanced in microgravity. This result agrees with Straub's [10] and Wan's [22] conclusions. However, the general trend of each wire behavior is similar to a first order system where the independent variable is heat flux and the final steady state ratio results in a value above unity. This either contradicts Straub's observation that heat transfer enhancement is lost at higher heat fluxes or the heat fluxes experienced in this

Table 4-3. Heat transfer coefficient fitted curves

	Equation	$q_0^{"}$ $(\frac{kW}{m^2})$	τ $(\frac{kW}{m^2})$
Single Wire	$1.14 - 0.51\exp(\frac{-q^{"} + q_0^{"}}{\tau})$	590	130
Three-Wire	$1.13 - 0.49\exp(\frac{-q^{"} + q_0^{"}}{\tau})$	310	230
Four-Wire	$1.13 - 0.59\exp(\frac{-q^{"} + q_0^{"}}{\tau})$	390	120

experiment were not high enough to see the same behavior. Additionally, the similarity of the first order time constants for the single and four-wire geometries, shown in Table 4-3, further illustrates the similarity in the heat transfer experienced by the two geometries.

3.4.4. Relative Bubble Area Analysis Method

While the majority of nucleate boiling experiments record visual data, the extent to which this data is used is often limited to qualitative observations. It would be of interest to correlate heating element temperature measurements to bubble dynamics from the visual recording. Typically, these types of correlations would come from bubble diameter or bubble number measurements which can be difficult and timely to gather for multiple frames of video and multiple tests. Therefore, there is a need for a method of data reduction to allow for the quick and accurate analysis of visual data between similar tests with varying system parameters.

A new method of relative bubble area analysis has been developed to fit this need. This method has proven very useful in the comparison of overarching trends between tests with varying system parameters and the indication of specific sections of video which may contain interesting dynamics to be analyzed further. The method simply sums the number of pixels in a particular greyscale frame that have changed since a designated initial frame. This initial frame contains the pixel values for the background of the video and the formation of bubbles changes

these values. A threshold value is used to decide how much a pixel value needs to be changed to be counted in an effort to balance the presence of false negatives and false positives. Therefore this method does not contain information on absolute bubble diameters or bubble counts but does provide a measure of how much bubble area is present relative to other tests and is an approximation of the volume of vapor formed. Figure 3-8b-c shows a representative frame from the video for a heat flux of 790 kW/m^2 experienced by the single wire, where the white pixels in Figure 3-8c are ones that were counted in the summation for that frame, while Figure 3-8a shows the initial frame used in the relative bubble area analysis method. Equation (3) provides a description of the algorithm used in the relative bubble area analysis, for reference.

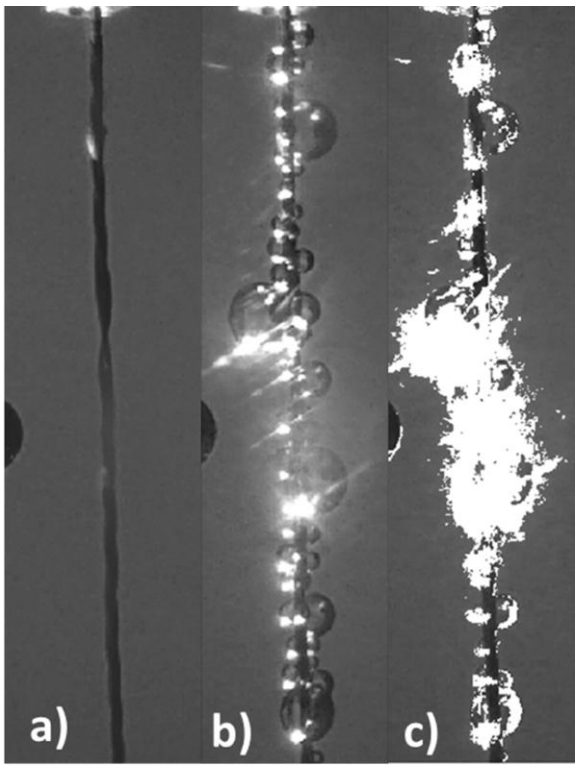

Figure 3-8. Relative bubble area analysis with changed pixels registered by method. Initial frame (a), subsequent frame (b), and changed pixel values changed to white (c).

$$[\text{Frame}]_{i,j}^{n} - [\text{Frame}]_{i,j}^{\text{initial}} \begin{cases} > \text{threshold, count pixel} \\ < \text{threshold, ignore pixel} \end{cases} \quad (3)$$

While some pixels are counted along the thermocouples to the left of the wire and some of the edges the bubbles are not counted, the threshold value of 45 was chosen to reduce the occurrence of both of these sources of error. Uncertainty of this method is largely due to false positives from light reflecting off the thermocouple beads and wire terminals. For the current experiment the uncertainty is as little as 1.5% and as great as 5%, but could be further reduced by elimination of all other objects except the wire from the interrogation window.

This method was run for each video from the current experiment producing graphs similar to that of Figure 3-9 (top), which plots the number of changed pixels for each frame of the video. Typically, within a few tenths of a second after powering the heating element, the water violently trips into boiling causing a rapid formation and departure of bubbles seen as the sharp spike in Figure 3-9a. Following this spike and as the wire temperature rises to the steady state boiling temperature, the relative bubble area increases to a maximum value, typically after about 5-10 seconds of boiling. At this point, the majority of tests show a steady decrease in relative bubble area seen around 10-15 seconds of boiling. After investigation of the video, it is apparent that this decrease is due to the formation of jet flows of small bubbles (Figure 3-9d). Since these small, high velocity bubbles are less visible, these jets make minor contributions to the relative bubble area summation and represent a decrease in changed pixels.

It is interesting to observe the steadiness of the heating element temperature from Figure 3-10 (dotted) despite the obvious changes in bubble dynamics seen in Figure 3-10 (solid). This further illustrates the conclusion that even though heat transfer has reached a steady state (in terms of wire temperature), that bubble dynamics can continue to change. The relative bubble area analysis is able to provide a quantitative way to verify this conclusion.

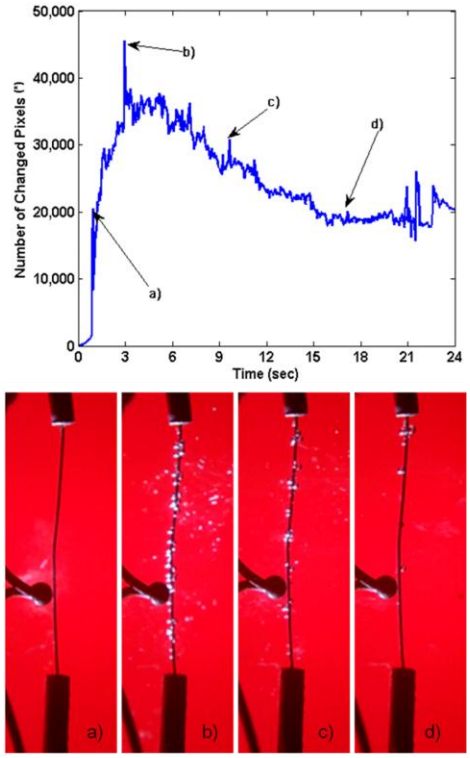

Figure 3-9. Relative bubble area analysis showing bubble growth behavior.

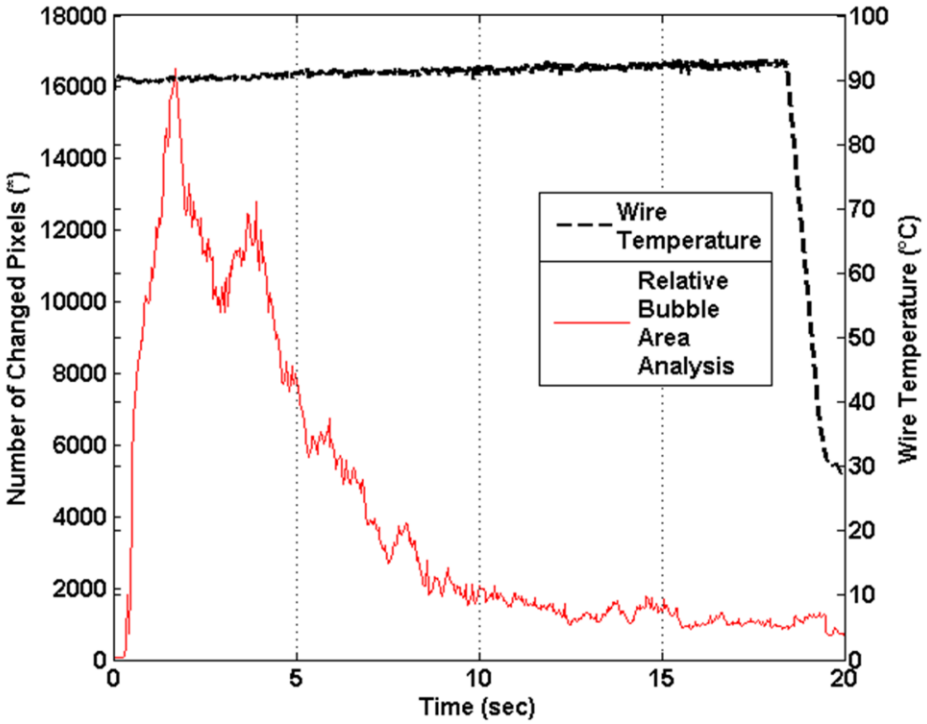

Figure 3-10. Wire temperature versus bubble dynamics (from relative bubble area analysis).

Figure 3-11 shows the relative bubble area plots from single wire videos for each of the five heat fluxes. As the power dissipated by the wire increases, the relative number of changed pixels increases until it reaches a turning point at a heat flux of 790 kW/m^2. This behavior reflects the behavior of the boiling videos which show a dominance of isolated bubbles at lower heat fluxes and a dominance of jet flows (which were difficult to detect with the lighting of the experiment) at the higher heat fluxes. Boiling did not occur at a heat flux of 600 kW/m^2 and the relative bubble area method represents heat distortion of the superheated water around the wire, which registers as changed pixels.

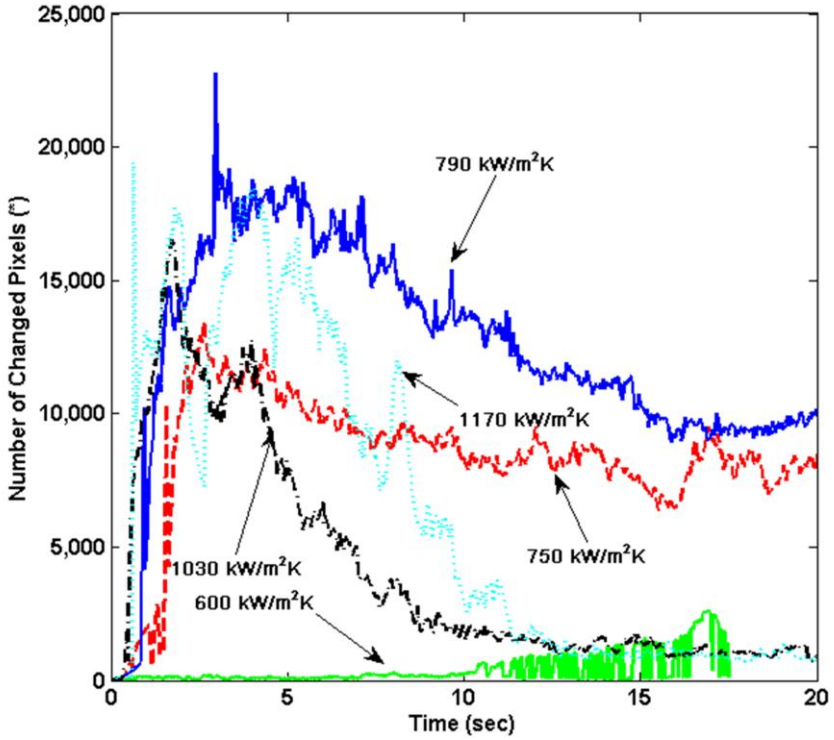

Figure 3-11. Relative bubble area analysis heat flux comparisons for single wire.

Figure 3-12 shows the relative bubble area plots for the third experimental condition for each of the three geometries and shows that the three-wire geometry has a greater number of changed pixels than both the single and four-wire geometries. This trend reflects the qualitative observation seen in the boiling videos that the three-wire geometry forms larger isolated bubbles and fewer jet flows, which is a characteristic of lower heat fluxes. Furthermore, Figure 3-12 shows similar results for the bubble dynamics of the single and four wire geometries, which further supports the conclusion that as the number of wires in the twist increases, the more closely the wire twist approaches the behavior of a single wire. This difference could be because the three-wire geometry has higher local heating temperatures which could be a mechanism for production of isolated bubbles rather than jets or could be due to the lower heat fluxes experienced by the three-wire geometry.

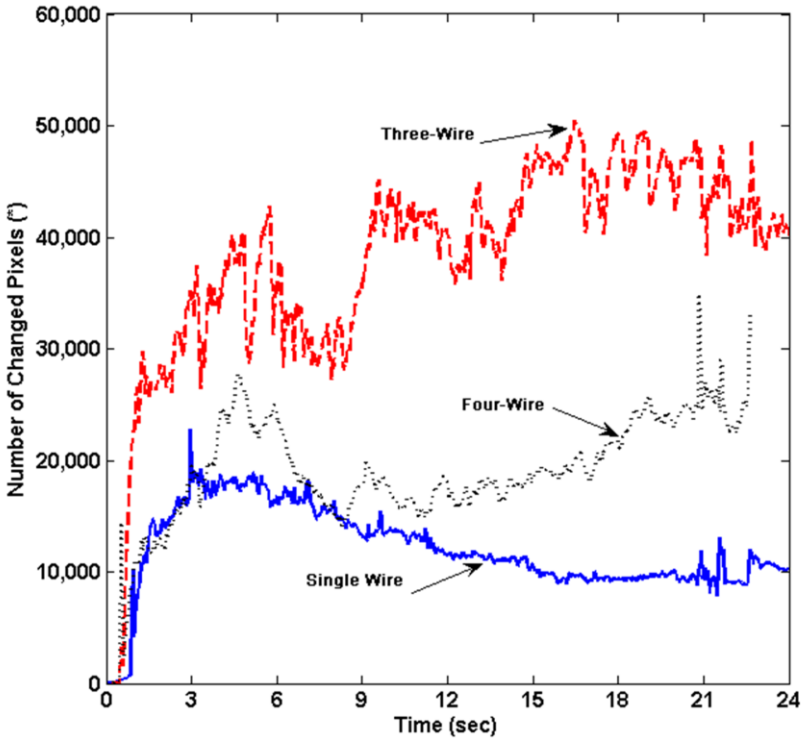

Figure 3-12. Relative bubble area analysis wire geometry comparison for the third experimental condition.

3.5. Conclusions

Based on the results and analysis of this parabolic flight experiment, the following conclusions can be made:

1. Twisting wires reduces onset heat flux and provides a lower average heater temperature during superheating due to local superheating in the wire crevices. This average superheated wire temperature difference can be as large as 45 °C between the single and three-wire geometries. The water temperature profile at the bubble onset indicates that a certain amount of water, in this experiment 50 μm from the surface, needs to be heated to above saturation temperature in order to initiate and generate a burst of bubbles.

2. Single wire boiling in microgravity is up to 15% more effective than boiling in terrestrial gravity. It is expected that wire twisting will continue to experience heat transfer coefficient enhancements in microgravity at higher heat fluxes.

3. The relative bubble area analysis method is able to quantitatively approximate the characteristics of boiling behavior of video data from boiling experiments. System behavior such as onset bubble formation and departure as well as modes of boiling are detected using the method. Application of the method across similar experimental setups allows the effects of bubble dynamics to be compared across system parameter variations, such as heat flux and surface geometries in the current experiment.

4. In microgravity, the three-wire geometry experiences greater heat transfer enhancements than the four-wire geometry because of lower onset heat flux, shortened superheating periods, and a lower average wire temperature due to local superheating.

3.6. References

[1] J. Straub, Boiling heat transfer and bubble dynamics in microgravity, in: J. Hartnett, T. Irvine, Y. Cho, G. Greene (Eds.), Advances in Heat Transfer, Elsevier, London, 2001, pp. 57-172.

[2] V.K. Dhir, Mechanistic prediction of nucleate boiling heat transfer – Achievable or a Hopeless Task?, Journal of Heat Transfer 128 (1) (2006) 1-12.

[3] P. Di Marco, W. Grassi, Motivation and results of a long-term research on pool boiling heat transfer in low gravity, International Journal of Heat and Fluid Flow 30 (2002) 751-760.

[4] M. Zell, J. Straub, A. Weinzieri, Nucleate pool boiling in subcooled liquid under microgravity – results of TEXUS experimental investigations, in Proceedings of the 5th European Symposium on Material Sciences under Microgravity, EPA SP-222, Schloss Elmau, Germany, 5-7 November 1984, pp. 327 333.

[5] G.R. Duursma, F. Jiang, K. Sefiane, S. Duff, H. Beji, On the effects of thermocapillary driven oscillations on bubble growth during boiling of FC-72 on a thin wire, International Journal of Thermal Sciences 50 (10) (2011) 1809-1819.

[6] S.X. Wan, J.F. Zhao, Pool boiling in microgravity: recent results and perspectives for the Project DEPA-SJ10," Microgravity Science and Technology 20 (3) (2008) 219-224.

[7] S. Petrovic, T. Robinson, J.L. Ross, Marangoni heat transfer in subcooled nucleate pool boiling, International Journal of Heat and Mass Transfer 47 (23) (2004) 5115-5128.

[8] S. Wan, J. Zhao, G. Liu, Dynamics of discrete bubble in nucleate pool boiling on thin wires in microgravity, Journal of Thermal Sciences 18 (1) (2009) 13-19.

[9] O. Kannengieser, C. Colin, W. Bergez, Pool boiling with non-condensable gas in microgravity: results of a sounding rocket experiment, Microgravity Science Technology 22 (3) (2010) 447-454.

[10] J. Straub, Highs and lows of 30 years research of fluid physics in microgravity, a personal memory, Microgravity Science and Technology 18 (3-4) (2006) 14-20.

[11] J. Straub, Bubble – bubbles – boiling, Microgravity Science and Technology 16 (1) (2005) 242-248.

[12] J. Straub, M. Zell, B. Vogel, What we learn from boiling under microgravity, Microgravity Science and Technology 6 (1993) 239-247.

[13] C.K. Huang, C.W. Lee, C.K. Wang, Boiling enhancement by TiO2 nanoparticle deposition, International Journal of Heat and Mass Transfer 54 (23-24) (2011) 4895-4903.

[14] Z.G. Xu, Z.G. Qu, C.Y. Zhao, W.Q. Tao, Pool boiling heat transfer on open-celled metallic foam sintered surface under saturation condition, International Journal of Heat and Mass Transfer 54 (17-18) (2011) 3856-3867.

[15] C.H. Li, T. Li, P. Hodgins, C.N. Hunter, A.A. Voevodin, J.G. Jones, G.P. Peterson, Comparison study of liquid replenishing impacts on critical heat flux and heat transfer coefficient of nucleate pool boiling on multiscale modulated porous structures, International Journal of Heat and Mass Transfer 54 (15-16) (2011) 3146-3155.

[16] Y. Fukada, I. Haze, M. Osakabe, The effect of fouling on nucleate pool boiling of small wires, Heat Transfer-Asian Research 33 (5) (2004) 316-329.

[17] M.C. Chyu, A.M. Mghamis, Nucleate boiling on two cylinders in line contact, International Journal of Heat and Mass Transfer 34 (7) (1991) 1783-1790.

[18] J. Xu, W. Zhang, Effect of pulse heating parameters on the microscale bubble dynamics at a microheater surface, International Journal of Heat and Mass Transfer 51 (1-2) (2008) 389-396.

[19] J.M. Delhaye, J.B. McLaughlin, Appendix 4: report of study group on microphysics, International Journal of Multiphase Flow 29 (7) (2003) 1101-1116.

[20] X. Quan, G. Chen, P. Cheng, A thermodynamic analysis for heterogeneous boiling nucleation on a superheated wall, International Journal of Heat and Mass Transfer 54 (21-22) (2011) 4762-4769.

[21] H.W. Coleman, W.G. Steele, Experimentation, Validation, and Uncertainty Analysis for Engineers, third ed., John Wiley & Sons, Hoboken, NJ, 2009 pp. 121-184.

[22] J.F. Zhao, G. Liu, S.X. Wan, N. Yan, Dynamics of discrete bubble in nucleate pool boiling on thin wires in microgravity, Microgravity Science and Technology 20 (2) (2008) 81-89.

CHAPTER 4

JET FLOWS OF MICRO-BUBBLES IN THIN WIRE, SUBCOOLED BOILING IN MICROGRAVITY

This chapter is a paper[a] submitted as a journal article in the Journal of Heat Transfer, pending review. All permissions to using this paper as a part of this thesis are contained in Appendix A.

4.1. Abstract

A thin wire, subcooled boiling experiment was performed onboard an aircraft flying a parabolic trajectory as a means to provide microgravity conditions for improved observation of jet flow phenomena and to investigate their behavior in the absence of buoyant forces. A new mode of jet flows was observed in microgravity which accounts for the high heat fluxes measured on the wire heater. This new micro-bubble jet flow is seen at medium to high heat fluxes and is characterized by a region of the wire that forms multiple jet columns which contain micro-bubbles. These columns flow together and penetrate tens of millimeters into the bulk fluid. Bubble behavior on the wire was observed to progress from a dominance of larger isolated bubbles on the wire to a dominance of micro-bubble jet flows on the wire as heat flux was increased. There was also a time-dependent transition from a few isolated large bubbles to micro-bubble jet flow dominance for a set heat flux. A cross-correlation calculation provided velocities of micro-bubble in the flow, which were in the range of 4-14 mm/s. These velocities were used with convection correlations to show that fluid flows induced by jet flows are a significant contributor to the subcooled boiling heat transfer in microgravity, but are not the primary

[a] Coauthor: Heng Ban

contributor. Additionally, a relative bubble area analysis provides approximations of the direct contribution of these jet flows to the overall heat dissipation. These micro-bubble jet flows and the convection currents they induce have the potential to allow for sustained boiling to occur in microgravity at high heat fluxes.

4.2. Introduction

Although boiling has been studied extensively, the last 10 years have shown an increase in the literature concerning jet flow behavior because technological advances in optical measurements as well as the use of microgravity environments have allowed researchers to investigate the behavior of this phenomenon. Jet flows are of particular interest because it has been proposed that they are the mechanism that explains the high heat fluxes observed in nucleate boiling [1]. Because jet flows can be masked by natural convection under normal gravity, the absence of buoyancy forces in microgravity allows jet behavior to be studied with fewer influences. Additionally, the microgravity environment provides the ability to observe unique behavior of these boiling modes [1].

Jet flows are a separate, observed mode of boiling heat transfer (compared to standard bubble nucleation, growth, and departure), and many different modes of jet flows have been observed. Wang [2] characterizes several different modes of jets (high-energy liquid jet, fog-like jet, cluster-like jet, bubble-forming jet, bubble-bunch jet, and bubble-top jet) that are produced depending on the fluid, level of subcooling, and applied heat flux. A summary of these jet flows and their behavior is given by Peng [3]. Zhukov et al. [4] concludes that these jet flows, referred to as microjets, are the mechanism that are able to provide high heat fluxes and are formed because of oscillatory, localized destruction of a metastable, superheated boundary layer. There were three modes of these metastable liquid boundary layer destruction zones observed during his

experiment: zones that had vapor present but did not form a jet, zones that formed defocused jets, and zones that formed jets capable of penetrating a distance of tens of wire diameters into the fluid. Additional modes of subcooled nucleate boiling have been characterized, such as the multi-jet [5,6], large bubble, small explosive bubbles, and coexisting bubble boiling [7], with additional modes being possible; it is important to investigate each of their enhancements on heat transfer [8]. After characterization of these modes, the heat transfer performance of the coexisting bubble boiling was approximated as a sum of the large and small explosive bubble modes of boiling, based on their equilibrium currents [7]. The current study is able to confirm this method, but seeks to further investigate the contribution of each mode of bubbles in coexistent boiling through the use of a relative bubble area comparison. In this way, the amount of heat dissipated by jet flows can be compared to the amount of heat dissipated by isolated bubbles.

The development and characteristics of jet flows are greatly influenced by thermocapillary forces, which exist in subcooled boiling [4,9,10], although Straub observes that these jet flows participate more as a mass transport mechanism than a heat transfer mechanism [11]. Conversely, Shekriladze concludes that jet flows can have a pumping effect, which explains the high heat transfer rates observed, and that jet flows are generated due to non-uniformity of evaporation of the bubble when its growth remains in the layer with a high temperature gradient [12-14]. Lu investigated the development of bubble jet flows and characterizes them into three stages of waiting, burst, and stably developing stage, and he observed that the bubble jet flows exist on top of bubbles of radius 0.01 mm to 0.30 mm and extend into the flow 0.5-2.0 mm [15]. Velocities of the fluid pumped by this bubble top jet flow were on the order of 10-140 mm/s [16,17], while the velocity of the bubble sweeping along the wire was lower, 20-50 mm/s [18]. All of these velocities were measured in the very near-field of the wire, but their behavior into the bulk fluid was not investigated. The current study seeks to investigate the velocity of additional jet flows and their contribution to heat transfer.

Bubble velocities can be determined based on a cross correlation calculation between time sequential images of bubble movement, which is similar to particle image velocimetry (PIV). Traditional use of PIV involves a light sheet from a pulsed laser, a high speed camera, and tracer particles to match the motion of the fluid in question. In boiling experiments, bubbles can be directly visualized instead of additional tracer particles, and the resulting cross correlation computation represents bubble velocities, which may or may not represent fluid velocity. Use of traditional PIV in boiling research has resulted in velocity data for bubble growth and departure [19] and the development of bubble top jet flow [16,17]. Additionally, traditional PIV has been used to verify numerical models of bubble sweeping flows and the jet flows they trail [18,20]. Jet flows can be affected by the presence of non-condensable gases, and it has been observed that an increase in subcooling increases heat transfer and bubble sweeping velocity [21]. However, little work has been done to investigate the fluid motion of other modes of jet flows by means of traditional PIV or by a bubble image velocimetry. This could be due to the inability of tracer particles to accurately mimic these flows or the sensitivity of different modes to lighting conditions. The current project discusses a method based on a DaVis 7.2 PIV algorithm for the approximation of jet flow velocities of some of these other jet flow modes, which has not been investigated in the literature. The term PIV is used in the remainder of the paper to represent bubble image velocimetry.

This study intends to investigate the existence of additional modes of jet flows, quantify bubble dynamics and behavior to correlate their effect on heat transfer characteristics, study heat transfer behavior in microgravity, and study the velocities of additional jet flow modes and their effect on the bulk fluid. This has been done through the use of a microgravity environment to improve visibility of jet flows, visual recordings of boiling on thin wires at various heat fluxes, a relative bubble area analysis to compare vapor formation, and a cross correlation algorithm to measure the motion of small vapor bubbles existent in the jet flows of interest. The results

provide means to characterize jet flows, their dynamics, and their contribution to boiling heat transfer.

4.3. Experimental Setup

Two different sets of microgravity experiments, the first being a free float experiment and the second attached to the floor of the plane, were flown on an aircraft flying a parabolic trajectory. Each experiment used identical fluid chambers to provide similar initial conditions for boiling on thin wires. The free float experiment used fifteen fluid chambers where one-third contained a single 130 μm diameter platinum wire, another third contained a twist of three 76 μm diameter platinum wires, and the final third contained a twist of four 51 μm diameter platinum wires. The attached experiment used twenty fluid chambers where half contained a single 130 μm diameter platinum wire and the other half contained a twist of three 76 μm diameter platinum wires. All wire geometries are shown graphically in Figure 4-1a. Each wire was 1 cm long and was connected to the ends of two stainless steel rods by means of electrical terminals, which pinched the wires at the ends. These stainless steel rods protruded into the fluid chamber from the instrument panel and provided electrical power and structural support for the wire heater (Figure 4-1b, right). This instrument panel also had a ladder of four Type T thermocouples located below the heating wire to provide initial bulk temperatures and to measure the thermal response of the water away from the wire. Each fluid chamber (Figure 4-1b, left) contained 164 mL of deionized water that was degassed through boiling under a vacuum prior to the filling of the fluid chamber. Polycarbonate walls, an O-ring, and epoxy seals allowed for flexing of the sidewalls to reduce the effects of internal pressure changes due to vapor formation.

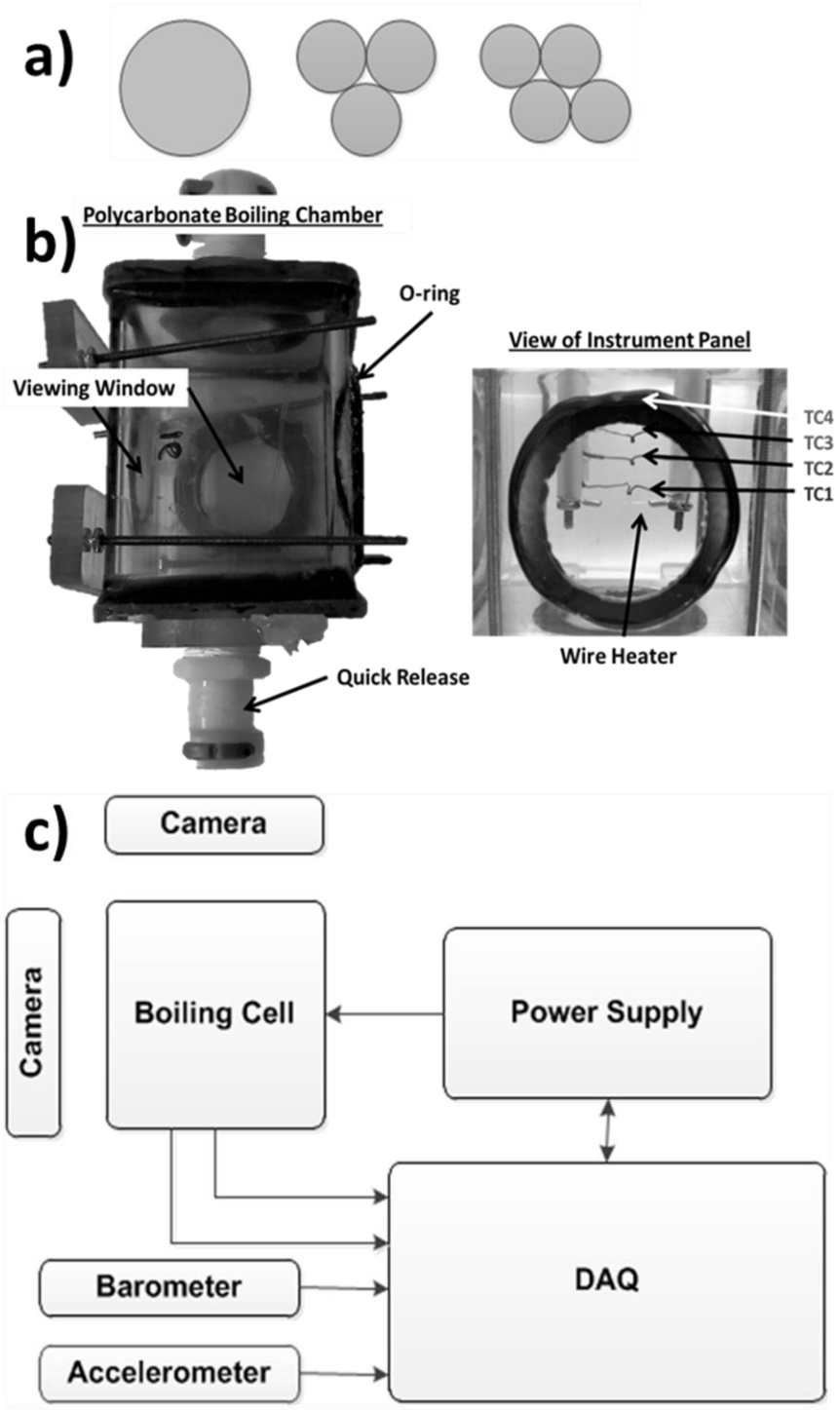

Figure 4-1. Experimental description. Wire cross-sections (a), fluid cell (b), system diagram (c).

During each microgravity parabola, the free float experiment tested three fluid cells, each with a different wire geometry, while the attached experiment tested two fluid cells. Operation of each experiment was the same and followed the schematic shown in Figure 4-1c. The data acquisition system would select one of eight pre-programmed constant current levels, which would then provide power from separate DC power supplies to each of the wire heaters. Voltage and current measurements of the wire heater were taken at approximately 10,000 Hz, with the average and standard deviation being recorded every 10 ms. Pressure and accelerometer measurements were taken in the same manner and resulted in an ambient pressure of about 82 kPa and an average acceleration near 10^{-2} g. Thermocouple measurements were taken at 75 Hz. Two orthogonal, high definition cameras provided image capture for each fluids cell, and through use of magnifying lenses, a pixel resolution of 14 µm x 14 µm was achieved.

The free floating experiment used two diffused red LEDs and one harsh white LED to provide a balance between visibility of both isolated bubbles and jets flows. Additionally, heat fluxes experienced by this experiment are in the low to medium range, 500 to 1200 kW/m^2. To compare the effect of lighting on jet flow visualization and to provide higher heat fluxes, the attached experiment used a single harsh white LED light and experienced heat fluxes from 500 to 5100 kW/m^2, at which point burnout occurs on the single wire. The extended surface area of the three-wire and four-wire twists cause a lower average heat flux to be dissipated for the same applied current/power as the single wire.

4.4. Results and Discussion

4.4.1. Jet Flow Characteristics

Because of the nature of jet flows, often visual data is the largest source for analysis of bubble behavior. Through high definition cameras and two lighting arrangements, a new mode of

jet flows was observed during subcooled, nucleate pool boiling in microgravity. This mode, referred to as micro-bubble jet, is characterized by the departure of very small bubbles in multiple columns which form as jets on a section of the wire and extend several centimeters into the bulk fluid. Although Lu's observed small explosive bubble boiling [7] is somewhat close to what was observed in this project, the increased size, form, and self-organization of the jet flows seen in the current study leads to the conclusion that this is a new mode of jet flow. Potential explanations for this mode of jet flows are the high degree of subcooling (70 °C), lower than atmospheric pressures, harsh LED lighting experienced during the attached experiment for visibility, wire twisting, and the microgravity testing environment. These conditions allow for non-uniform behavior near the heating wire and provide better illumination for vapor bubble visibility. Additionally, the absence of buoyant forces allows the departed bubbles to remain in the field of view longer.

Observations of the micro-bubble jet flow show the departure of small vapor bubbles, on the order of 100 μm, directly from the wire. A 1-2 mm long region of the wire forms multiple columns of these small bubbles, which combine and depart from the wire with a combined jet diameter of 3-4 mm. This is in contrast to the thin plumes that are seen above bubble top jet flows during the same experiment, which have diameter on the order of tens of microns. With these larger diameter combined jet flows and a flow consisting of liquid and vapor cloud, the observed velocities are expected to be lower than velocities that have been reported for other types of jet flows [16-18]. The microgravity environment allows the combination of jet flows into the bulk fluid to be seen when buoyancy effects would obscure these self-induced flows. Additionally, the three-wire geometry is observed to form micro-bubble jet flows more readily than the single wire, but the single wire is more likely to form nucleation jets like those investigated by Christopher and Wang [22]. During the few instances when micro-bubble jet flows were observed on the

single wire, the bubbles were smaller and less visible, similar to Lu's observations, and the flows did not combine like the flows observed on the three-wire.

At heat fluxes near the minimum onset heat flux to initiate boiling, these micro-bubble jet flows are non-existent and bubble behavior is dominated by isolated bubble production (Figure 4-2a). As heat flux increases, the number and intensity of jet flows increases until the wire is saturated with them (Figure 4-2b and c). As the heat flux approaches the critical heat flux, large isolated bubbles begin to form concurrently with these micro-bubble jet flows and eventually led to burnout on the single wire (Figure 4-2d). This transitional behavior based on heat flux changes mimics that seen by Lu [7] with the addition of the reemergence of large, isolated bubbles near critical heat flux (Lu did not investigate the behavior near critical heat flux).

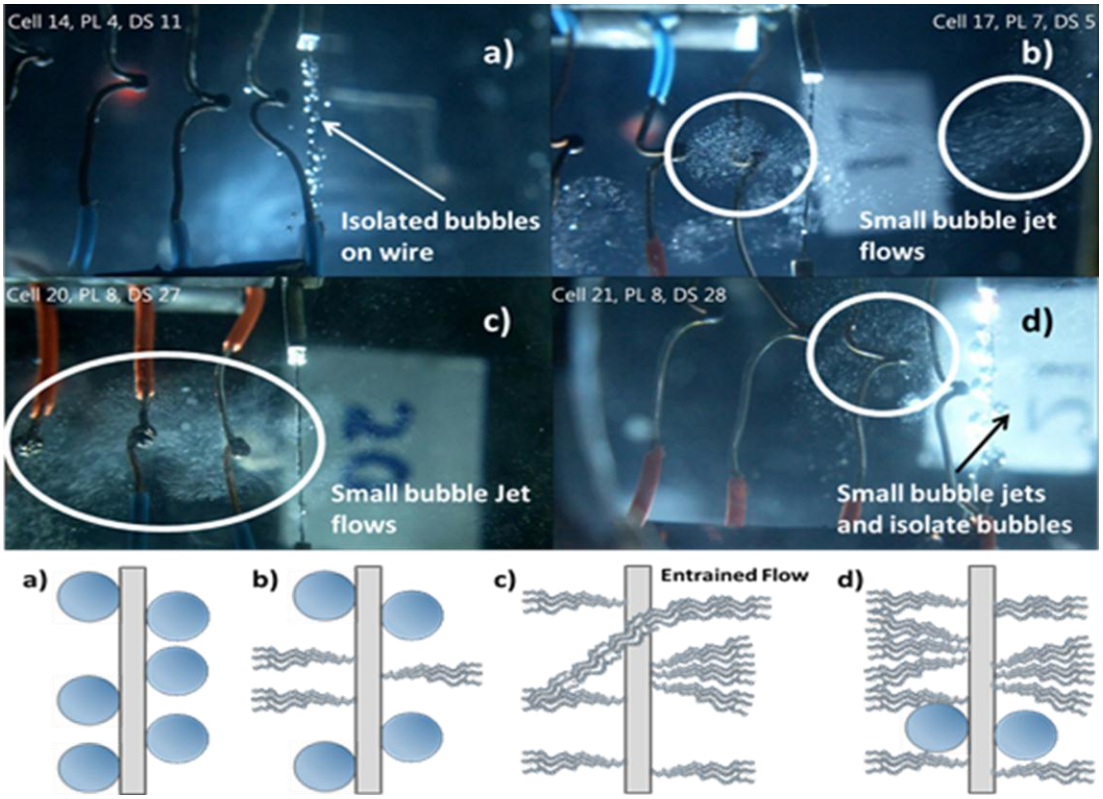

Figure 4-2. Boiling behavior of wires. Low heat flux – three-wire (a) high heat flux– three-wire (b and c), burnout – single wire (d).

In addition to a heat flux driven transition, a time dependent transition is also observed. For a given heat flux where jet flows are seen, the initial behavior of the wire is to have a rapid formation and departure of fine vapor bubbles (Figure 4-3 t=33ms). Shortly after this event, isolated bubbles of similar size to the wire appear on the majority of the wire, but several micro-bubble jets appear at locations away from the isolated bubbles (Figure 4-3 t=2.4s). As boiling continues, these jet flows interact to form a flow pattern drawing fluid and vapor away from the wire, and the presence of isolated bubbles on the wire decreases until the dominant bubble behavior is micro-bubble jets (Figure 4-3 t=16.7s). Finally, this induced fluid flow entrains all visible vapor bubbles departing the wire and results in an increase of bulk fluid temperature, as registered by the thermocouple ladder. This column of vapor and fluid is able to penetrate into the bulk fluid and maintain a continuous flow, upon completion of the transitional behavior. The mechanism behind this transient behavior has yet to be determined.

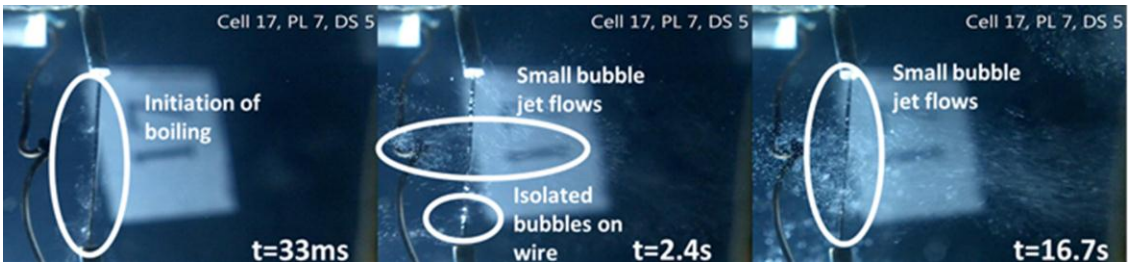

Figure 4-3. Transition to micro-bubble jet dominance over time for a given heat flux.

Because the unique surface geometry of the three-wire twist provides more external area for the same cross-sectional area, the heat flux dissipated by the three-wire is lower than the single wire for the same power supplied to the heater. However, the three-wire geometry is more likely to form micro-bubble jets at lower heat fluxes, while the single wire geometry more readily forms nucleation and bubble top jets at a similar heat flux. As both wire geometries approach critical

heat flux, both geometries exhibit micro-bubble jet flows. This behavior was seen during both experiments and leads to the conclusion that the micro-bubble jet flow mode exists at medium to high heat fluxes, whether on the global scale of the wire or at localized superheating regions in the crevices of the three wire.

4.4.2. Heat Flux Characteristics Through Relative Bubble Area Analysis

In an attempt to better quantify video data, a relative bubble-area analysis method was developed. This method approximates the total volume of vapor by looking at the area a bubble occupies relative to a frame of video where the bubble is absent, and the method provides a way to relate bubble behavior and dynamics to heat transfer behavior. The basic operation of this method is to find a reference point on each image, which was the farthest thermocouple in this experiment. This reference point is then used to create a stable interrogation window that includes the wire and approximately 2 mm of the adjacent fluid. Each subsequent image (Figure 4-4a) is then subtracted from an initial frame (Figure 4-4b), where there is no boiling, and if a pixel intensity has changed more than a threshold value, that pixel is counted towards the relative bubble-area (Figure 4-4c). The threshold value is chosen to reduce false positives due to glare off the wire terminals and thermocouple beads. Use of this method allows the vapor behavior of an entire video to be represented in a single graph and the relative effects of system parameters to be compared across different sets of data.

As Straub [23] observed, visualization of jet flows is greatly influenced by lighting conditions. Because the relative bubble area method relies upon the ability to see bubbles in the interrogation window, vapor bubbles that are not visible in jet flows are not counted in the relative bubble area. The diffused lighting in the free float experiment limited the visibility of some jet flows on the single and four-wire geometries. However, it was concluded that the jet flows existed because isolated bubble trajectories were affected by some invisible flow field.

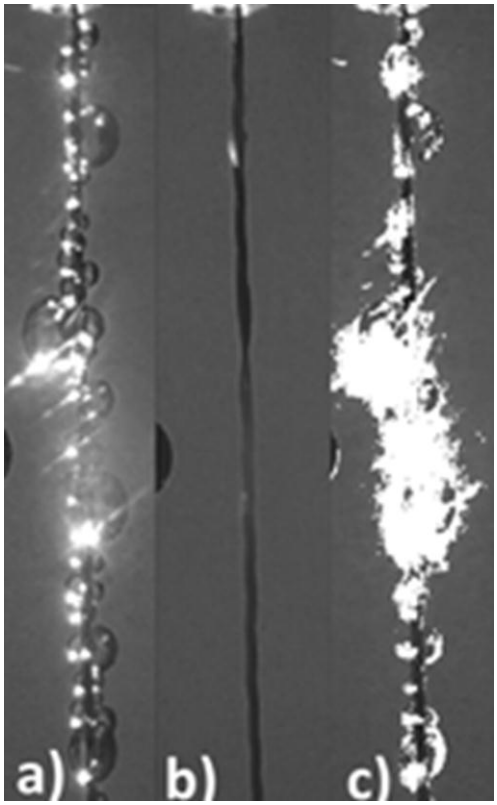

Figure 4-4. Relative bubble area analysis frames. Interrogation frame (a), initial frame (b), changed pixels in white (c).

This flow field was assumed to be due to the jet flows that were not visible. When jets flows do not register in the relative bubble area, a decrease in the number of large bubble generation and departure can be related to the development of jet flows. To illustrate this progression, Figure 4-5 t=0s shows the wire before boiling is initiated and Figure 4-5 t=1.8s shows the dominance of isolated bubbles on the wire. Figure 4-5 t=6s shows that the number of isolated bubbles has decreased, and invisible jet flows have formed. Figure 4-6 (top) shows the heat flux experienced by the wire, while Figure 4-6 (bottom) shows the results of the relative bubble-area analysis, which shows a decrease in changed pixels (normalized to the maximum number of changed pixels) starting at about 5 seconds. This further illustrates the time transitional behavior of these

jet flows. This behavior was seen on the single wire at all heat flux conditions where boiling occurred, but the four-wire twist had this general behavior only at higher heat fluxes. The three-wire twist did not show this behavior because the heat fluxes it experienced during the free float experiment did not transition to micro-bubble jets and remained mostly in the isolated bubble mode. The percentage of pixels shown by the relative bubble area of Figure 4-6 drops below 20% but the heat flux remains constant, meaning that approximately 80% of the vapor being produced by the wire is now being dissipated by jet flows (assuming that the same area of vapor is being produced).

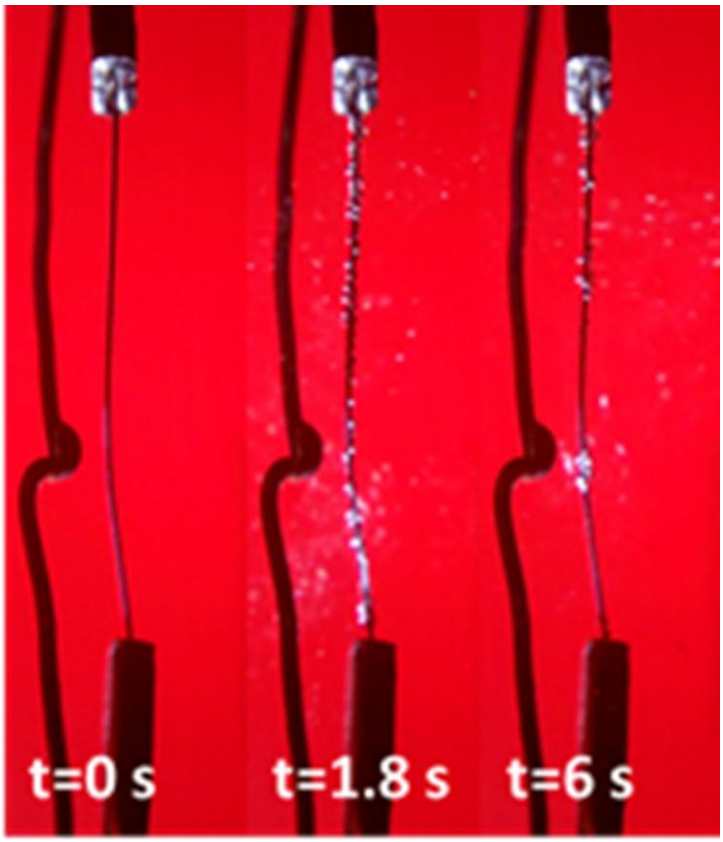

Figure 4-5. Jet flow transition behavior as observed with diffused lighting of free float experiment.

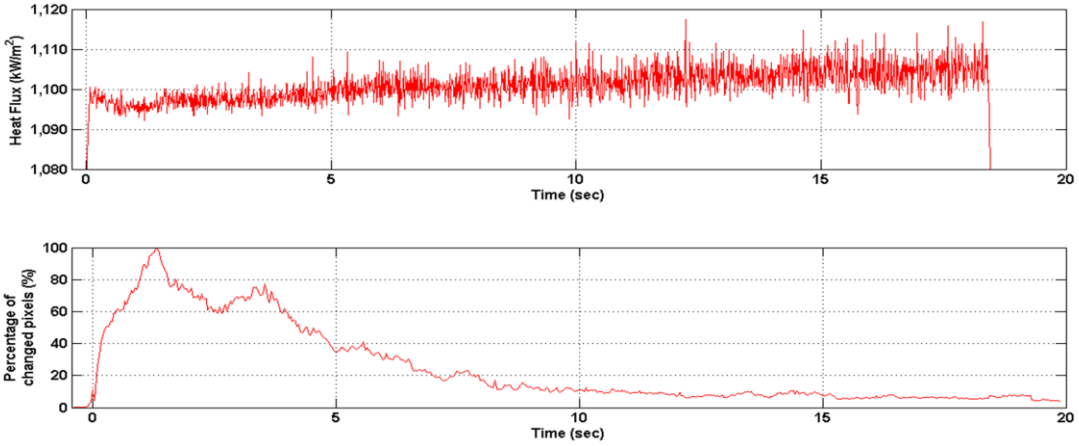

Figure 4-6. Heat flux dissipated compared to percentage of changed relative bubble area pixels, normalized to maximum number of changed pixels.

Equation (1) gives Lu's approximation [7], which seeks to approximate the overall heat flux for coexisting boiling using heat fluxes where only large bubble and micro-bubble boiling are present.

$$q^{"} = q^{"}_{se} + \frac{q^{"}_{le} - q^{"}_{se}}{T_{le} - T_{se}}(T_w - T_{se}) \quad (1)$$

This approximation was applied to data from the free floating experiment as references for the heat fluxes for the small and large bubble boiling, and results showed that this approximation is within 1% of experimental values of the measured heat flux (1030 kW/m^2) where coexisting boiling was observed. However, this method provides no estimate of the contribution of each mode of boiling to the overall dissipated heat flux. Using the relative bubble area analysis results shown in Figure 4-6, the resulting heat flux dissipated by the jet flows during coexisting boiling was estimated to be 824 kW/m^2, which is 80% of the total heat flux dissipated by the wire. This approximate value is larger than the onset heat flux for a single wire, which suggests that jet flows can dissipate more heat than isolated bubbles and are an important contributor to heat transfer. Additionally, Figure 4-6 illustrates the time transition behavior mentioned previously.

4.4.3. Particle Image Velocimetry Results and Heat Transfer Response

To provide an approximation of velocities experienced during micro-bubble jet flows, a PIV-derived method was applied to the boiling video images, after the background of images were removed by means of a pixel averaging algorithm. Use of a harsh LED light, rather than a pulsed laser, lower frame rate cameras, and the microgravity environment allow the micro- bubbles in the jet flow to be visible. As mentioned previously, the diffused lighting of the free floating experiment reduced the visibility of these micro-bubble jets. Rather than using tracer particles to mimic the flow, the vapor bubbles of the jet flows are treated as the particle to be correlated across picture frames because of their clear visibility and their active participation in the flow of interest. Although the planar flow assumption needed to allow for cross correlation is not valid for all bubbles visible in the flow, the results of this method agree within ±2 mm/s according to manual vapor bubble tracking. Typical velocities of these micro-bubble jet flows are on the order of 4 mm/s to 14 mm/s (Figure 4-7a). To approximate the maximum contribution of single-phase convection due to these induced flows, the maximum observed velocity was used in a circular cylinder in crossflow correlation, Eq. (2) [24,25].

$$\overline{Nu}_D = 0.3 + \frac{0.62 Re_D^{1/2} Pr^{1/3}}{(1+(0.4/Pr)^{2/3})^{1/4}} \left[1 + \left(\frac{Re_D}{282{,}000}\right)^{5/8}\right]^{4/5} \quad (2)$$

With the resulting average heat transfer coefficient, the maximum heat flux that single-phase convection could dissipate in the particular experiment was 580 kW/m^2, which is almost 31% of the measured heat flux dissipated by the entire wire. Because this approximation uses the maximum observed velocity of jet flow, it provides a likely overestimation of the heat transfer contribution of single-phase convection induced by these jet flows and supports the conclusion that the majority of heat is transferred through evaporation and condensation. However, it also shows that the contribution of single phase convection to the overall heat transfer cannot be considered negligible.

As the heat flux dissipated by the wire increases, the velocity of bubbles in the jet flow increases as more of the wire dissipates heat with these jet flows. Additionally, the jet flows are more likely to form into a bulk flow that penetrate centimeters into the bulk fluid and can cause mushroom headed flows. Velocities in these bulk flows are able to maintain a steady flow departing the wire. This cross correlation PIV technique allows the departure velocity of these jets flows to be approximated as well as the bulk flow induced by theses jets. It also shows the entrainment caused by the departure of combined jets flows as vapor from the left of the wire in Figure 4-8 is pulled back to the right.

It is important to investigate the heat transfer of these jets in the bulk fluid, in addition to the convective heat transfer near the wire due to micro-bubble jet flows, which has already been investigated earlier in this paper. To do this, PIV measurements were used to approximate the convective heat transfer to the second thermocouple bead on the thermocouple ladder by a single jet flow. It is assumed that this thermocouple is representative of the thermal response of the bulk fluid because it is located several millimeters away from the wire. In this analysis, the flow properties and fluid temperature were assumed to be an average of the saturated vapor and bulk fluid properties and are given as $\rho = 796\frac{kg}{m^3}$, $Pr = 3.4$, $\mu = 4.3 \times 10^{-4}\frac{N{\cdot}s}{m^2}$, $\mu_s = 2.4 \times 10^{-4}\frac{N{\cdot}s}{m^2}$, $\nu = 4.4 \times 10^{-7}\frac{m^2}{s}$, $k = 0.32\frac{W}{m{\cdot}K}$. After curve fitting a velocity profile (curved line in Figure 4-7b), the average velocity of the jet flow was used to determine the Reynolds number of the flow, with the diameter of the thermocouple bead as the characteristic length. Then, treating the thermocouple bead as a sphere and using Whitaker's correlation for external flow, Eq. (3) [24,26], the Nusselt number and associated heat transfer coefficient were obtained.

$$\overline{Nu}_D = 2 + (0.4Re_D^{1/2} + 0.06Re_D^{2/3})Pr^{0.4}\left(\frac{\mu}{\mu_s}\right)^{1/4} \quad (3)$$

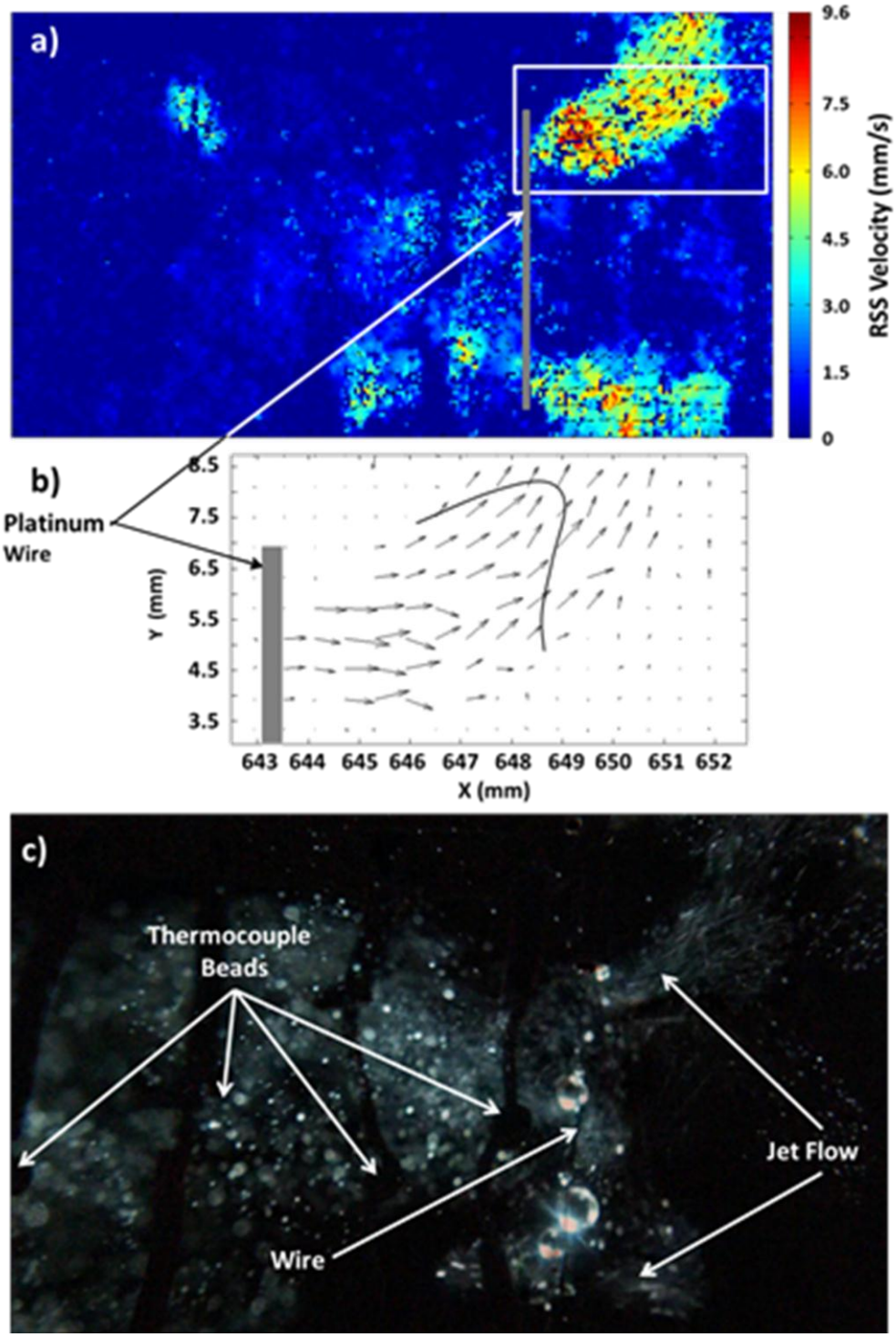

Figure 4-7. PIV results for high heat flux showing two micro-bubble jet flows (a), velocity profile fitted to velocity vectors by method (b) and source image (c).

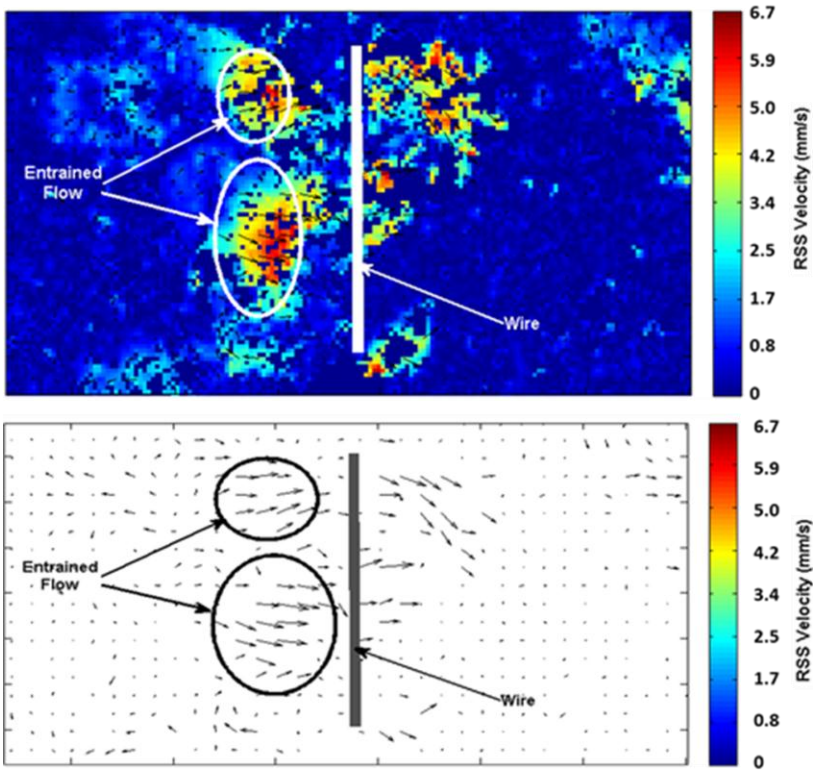

Figure 4-8. PIV results showing entrained flow with jet flows formed on the right side of the wire. Contour map of velocity magnitudes (top) and velocity vectors of flow (bottom).

Finally, the average heat flux that one jet flow transferred to the thermocouple was estimated by multiplying the heat transfer coefficient by the temperature difference between the measured thermocouple temperature and the average temperature of the jet, which was assumed to be the average of the saturation temperature and the bulk fluid temperature. The heat flux of the jet to the thermocouple was calculated to be 73 kW/m^2, which is almost 2% (±0.7% according to Monte Carlo uncertainty analysis) of the total measured heat flux dissipated by the wire heater. The heat transferred from the heater wire to the bulk flow is expected to increase with each additional jet that is produced by the wire. This further shows that although the majority of the heat dissipated by the heater is from phase change, the convective flows that are generated by jet

flows contribute significantly to the overall heat transfer of the system. This behavior in microgravity allows for sustainable convective flows to be established in place of natural convection currents. Although velocities of the micro-bubble jet are lower than initial departure velocities seen in literature, the combination and self-organization of the hot fluid and vapor columns allows them to be more constant as they penetrate further into the bulk fluid.

4.5. Conclusions

Based on analysis of both microgravity experiments, the following conclusions can be made:

1. A new mode of jet flows of subcooled boiling in microgravity is observed, which is characterized by self-organizing columns of micro-bubbles on a section of the wire. These flows can combine into a single flow that entrains bulk fluid and is capable of dissipating significant amounts of heat into the bulk fluid.

2. A time transitional behavior from large, isolated bubbles to micro-bubble jet flows was observed visually and by means of a relative bubble area method. This method, which sums the number of changed pixels across video frames, can also show that jet flows dissipate a larger percentage of the overall measured heat flux than the isolated large bubble growth and departure mode. These micro-bubble jet flows do not contribute to the relative bubble area if the lighting is unable to make them visible, and this decrease in relative bubble area for a given heat flux can approximate the percentage of heat dissipated by the jet flows.

3. Two modes of bubbles in boiling were observed to be a function of heat flux. The large, isolated bubbles are the dominant mode at low heat fluxes, but the mode of micro-bubble jet flows becomes the dominant bubble behavior on the wire at high heat fluxes. At medium heat fluxes, a coexisting mode of both isolated bubbles and micro-bubble jets is observed.

4. Using the bubbles produced in the micro-bubble jet flow as tracer particles gives good approximation of velocities when using the DaVis 7.2 PIV algorithm, despite the limitations and assumptions necessary to implement the cross correlation calculation in the current experiment. PIV measurements of micro-bubble jet flows give velocity magnitudes between 4-14 mm/s, which can be maintained at many tens of millimeters into the bulk fluid.

5. Using the maximum observed velocity and a cylinder crossflow correlation, the heat flux dissipated by single-phase convection was estimated to be < 30% of the heat flux dissipated by the wire heater. It is more likely that this value is closer to 10%-15%, but the results support the conclusion that the majority of the heat dissipated by the wire is through evaporation and condensation rather than the single-phase flow induced by jet flows. However, the contribution of jet flows to heat transfer is sufficiently significant that it should not be ignored.

4.6. References

[1] Peng, X.F., Wang, Z., and Lee, D.J., 2004, "Dynamic Behavior of Vapor Interface during Nucleate Boiling," J. Chin. Inst. Chem. Engrs., **35**(4), pp. 467-475.

[2] Wang, H., Peng, X.F., Wang, B.X., and Lee, D.J., 2002, "Jet Flow Phenomena During Nucleate Boiling," Intl. J. of Heat and Mass Transfer, **45**(6), pp. 1359-1363.

[3] Peng, X., 2011 , Micro Transport Phenomena During Boiling, first ed., Tsinghua University Press, Beijing, Springer, Heidelberg, pp. 60-91, Chap 4.

[4] Zhukov, S.A., Afanas'ev, S.Y., and Echmaev, S.B., 2003, "Concerning the Magnitude of the Maximum Heat Flux and the Mechanisms of Superintensive Bubble Boiling," Intl. J.of Heat and Mass Transfer, **26**(18), pp. 3411-3427.

[5] Shekriladze, I.G., 2006, "Discussion: 'Dynamics of Bubble Motion and Bubble Top Jet Flows from Moving Vapor Bubbles on Microwires' (Christopher, D.M., Wang, H., and Peng, X., 2005, Journal of Heat Transfer, 127, pp. 1260-1268)," J. of Heat Transfer, **128**(12), 1343-1344.

[6] Christopher, D.M., Wang, H., Peng, X., and Garimella, S.V., 2006, "Closure to 'Discussion: "Dynamics of Bubble Motion and Bubble Top Jet Flows from Moving Vapor Bubbles on Microwires" (Christopher, D.M., Wang, H., and Peng, X., 2005, Journal of Heat Transfer, 127, pp. 1260-1268)'," J. of Heat Transfer, **128**(12), 1344-1345.

[7] Lu, J.F., Peng, X.F., and Bourouga, B., 2006, "Nucleate Boiling Modes of Subcooled Water on Fine Wires Submerged in a Pool," Exper. Heat Transfer, **19**(2), pp. 95-111.

[8] Wang, H., Peng, X.F., Wang, B.X., and Lee, D.J., 2003, "Bubble Sweepin and Jet Flows During Nucleate Boiling of Subcooled Liquids," Intl. J. of Heat and Mass Transfer, **46**(5), pp. 863-869.

[9] Henry, C.D., Kim, J., and McQuillen, J., 2006, "Dissolved Gas Effects on Thermocapillary Convection During Boiling in Reduced Gravity Environments," Heat and Mass Transfer, **42**(10), pp. 919-928.

[10] Petrovic, S., Robinson, T., and Judd, R.L., 2004, "Marangoni Heat Transfer in Subcooled Nucleate Pool Boiling," Intl. J. of Heat and Mass Transfer, **47**(10), pp. 5115-5128.

[11] Straub, J., 2002, "Origin and Effect of Thermocapillary Convection in Subcooled Boiling: Observations and Conclusions from Experiments Performed at Microgravity," Annals of the New York Academy of Sciences, **974**, pp. 348-363.

[12] Shekriladze, I.G., 2003, "Comment on the paper by H. Wang, X.F. Peng, B.X. Wang, and D.J. Lee 'Jet flow phenomena during nucleate boiling' IJHMT 45 (6) (2002) 1359-1363," Intl. J. of Heat and Mass Transfer, **46**(14), pp. 2711-2712.

[13] Shekriladze, I.G., 1966, "On the Mechanism of Nucleate Boiling," Bulletin Academy of Science Georgian SSR, **41**(2), pp. 392-396 (English version: Technical Report NASA TM X-59398, 1967, pp. 1-10).

[14] Shekriladze, I.G., 1970, "On the Role of the 'Pumping Effect' of a Vapor Bubble Growing at the Wall During Nucleate Boiling," Problems of Convective Heat Transfer and Steam Purity, V.G. Ratiani, ed., Metsniereba Press, Tbilisi, pp. 90-97.

[15] Lu, J.F., and Peng, X.F., 2007, "Bubble Jet Flow Formation during Boiling of Subcooled Water on Fine Wires," Intl. J. of Heat and Mass Transfer, **50**(19-20), pp. 3966-3976.

[16] Wang, H., Peng, X.F., Christopher, D.M., Lin, W.K., and Pan, C., 2005, "Investigation of Bubble-top Jet Flow During Subcooled Boiling on Wires," Intl. J. of Heat and Fluid Flow, **26**(3), pp. 485-494.

[17] Wang, H., Peng, X.F., Lin, W.K., Pan, C., and Wang, B.X., 2004, "Bubble-top Jet Flow on Microwires," Intl. J. of Heat and Mass Transfer, **47**(14-16), pp. 2891-2900.

[18] Christopher, D.M., Wang, H., and Peng, X., 2005, "Dynamics of Bubble Motion and Bubble Top Jet Flows from Moving Vapor Bubbles on Microwires," J. of Heat Transfer, **127**(11), pp. 1260-1268.

[19] Cieslinski, J.T., Polewski, J., and Szymczyk, J.A., 2005, "Flow Field around Growing and Rising Vapour Bubble by PIV Measurement," J. of Visualization, **8**(3), pp. 209-216.

[20] Wang, H., Peng, X.F., and Christopher, D.M., 2005, "Dynamic Bubble Behavior during Microscale Subcooled Boiling," Chinese Physics Letters, **22**(11), 2881-2884.

[21] Christopher, D.M., Wang, H., and Peng, X., 2006, "Numerical Analysis of the Dynamics of Moving Vapor Bubbles," Intl. J. of Heat and Mass Transfer, **49**(19-20), pp. 3626-3633.

[22] Christopher, D.M., and Wang, H., 2007, "Mechanism for Nucleation Jet Enhancement of Nucleate Pool Boiling," J. of Enhanced Heat Transfer, **14**(3), pp. 209-221.

[23] Straub, J., 2000, "Microscale Boiling Heat Transfer under 0g and 1g Conditions," Intl. J. of Thermal Science, **39**(4), pp. 490-497.

[24] Incropera, F.P., Dewitt, D.P., Bergman, and T.L., Lavine. A.S., 2007, Fundamentals of Heat and Mass Transfer, sixth ed., John Wiley & Sons, Hoboken, NJ, pp. 433-434,625-631, Chap. 7&10.

[25] Churchill, S.W., and Bernstein, M., 1977, "A Correlating Equation for Forced Convection from Gases and Liquids to a Circular Cylinder in Crossflow," J. of Heat Transfer, **99**(2), pp. 300-306.

[26] Whitaker, S., 1972, "Forced Convection Heat Transfer Correlations for Flow in Pipes, Past Flat Plates, Single Cylinders, Single Spheres, and for Flow in Packed Beds and Tube Bundles," AIChE J., **18**(2), pp. 361-371.

CHAPTER 5

CONCLUSIONS

Boiling heat transfer in microgravity has been studied and the results of two microgravity experiments have been presented. The objectives proposed at the end of Chapter 1 have been met: boiling behavior in microgravity and terrestrial gravity has been observed; a two-dimensional, transient heat conduction model has been developed to explain wire twisting effects on bubble growth, superheating temperature, and onset conditions; the results from this numerical model have been confirmed with observed behavior during the microgravity experiment; and analysis methods to approximate jet flows contribution to heat transfer and characterize their behavior have been developed.

From the results presented in Chapter 3, several conclusions on the effect of surface geometry and heat flux can be made, in reference to onset and steady state conditions:

- Twisting thin wires together causes localized regions of superheating in the crevices of the twist. This can reduce the average superheating temperatures by as much as 45 °C when the superheating temperature of the three-wire is compared to the single wire superheating temperature.
- The two-dimensional, transient heat conduction equation was able to predict the temperature field near the wire. It was determined that a certain amount of water at a critical distance from the wire, in this experiment 50 μm normal from the wire surface, needs to be heated to above saturation temperature in order to initiate and generate a burst of bubbles. This effect was more pronounced on the three-wire twist than on the four-wire twist, largely because the three-wire maintained higher temperatures at farther

distances from the wire. Additionally, the three-wire twist reduced the time at which the wire was above saturation temperature.

- In general, the three-wire twist experienced greater heat transfer enhancements due to shorter superheating durations, lower average heater temperature, and lower onset heat fluxes. This is of particular importance in microgravity because of the ineffectiveness of heat transfer prior to boiling initiation.

Chapter 3 and Chapter 4 investigated the use of a relative bubble area analysis method and a cross-correlation method based on particle image velocimetry (PIV) in boiling analysis. The following conclusions were made:

- Through use of the relative bubble area, the behavior of bubbles across multiple frames of video was able to be represented graphically. In this way, bubble behavior such as onset, mode of boiling, heat flux transitional behavior, and time transitional behavior were captured qualitatively.
- PIV results and convective correlations used support the conclusion that jet flows and the convective flows they induce, can provide a significant contribution to boiling heat transfer but are not the major contributor. The major contributor is the evaporation and condensation of vapor bubbles.
- Additionally, the relative bubble area method, with a diffused lighting environment, was able to approximate the heat flux dissipated by jet flows (by their formation and induced convection) and show that heat flux dissipated by jet flows is greater than heat flux dissipated by isolated bubble growth and departure. This helps explain why the behavior of boiling at high heat fluxes is dominated by jet flows prior to reaching critical heat flux.
- These methods also helped characterize a new jet flow mode, designated as micro-bubble jet flow, which consists of small vapor bubbles on the order of 100 μm that depart from a

section of the wire and combine to form a jet. These flows penetrate tens of millimeters into the bulk flow and have velocities between 4-14 mm/s.

In summary, sustained pool boiling in microgravity is possible and can experience heat transfer enhancements, in some instances. However, further research is needed to develop a mechanism based model to predict boiling behavior across a variety of systems. This further research includes application of the bubble image velocimetry with a pulsed laser sheet to the micro-bubble jet flow and other jet flow modes and CFD modeling of single phase fluid flow and the associated heat transfer characteristics based on velocity measurements. Additionally, the relative bubble area analysis method can be further refined to provide a more qualitative representation of bubble volume through incorporation of video data from the other orthogonal camera and reduction of false positives.

APPENDICES

APPENDIX A. PERMISSION LETTERS

February 25, 2012

Troy R. Munro
21 Aggie Vlg Apt C
Logan, UT 84341
801-558-4780

Dear Justin Koeln :

I am preparing my thesis in the Department of Mechanical and Aerospace Engineering at Utah State University. I hope to complete my degree in the spring of 2012.

I am requesting your permission to include the attached material as shown. I will include acknowledgments and/or appropriate citations to your work as shown and copyright and reprint rights information in a special appendix. The bibliographical citation will appear at the end of the manuscript as shown. Please advise me of any changes you require.

Please indicate your approval of this request by signing in the space provided, attaching any other form or instruction necessary to confirm permission. If you charge a reprint fee for use of your material, please indicate that as well. If you have any questions, please call me at the number above.

I hope you will be able to reply immediately. If you are not the copyright holder, please forward my request to the appropriate person or institution.

Thank you for your cooperation,

Troy R. Munro

I hereby give permission to Troy R. Munro to reprint the requested article in his thesis, with the following acknowledgment:

Munro, T.R., Koeln, J.P., Fassmann, A.W., Barnett, R.J., and Ban, H., 2012, "Surface Geometry Effect on Bubble Onset in Microgravity Pool Boiling," Manuscript submitted for publication to International Journal of Heat and Mass Transfer.

Signed: Justin Koeln

Date: 2-27-12

Fee: _____

February 25, 2012

Troy R. Munro
21 Aggie Vlg Apt C
Logan, UT 84341
801-558-4780

Dear Andrew Fassmann:

I am preparing my thesis in the Department of Mechanical and Aerospace Engineering at Utah State University. I hope to complete my degree in the spring of 2012.

I am requesting your permission to include the attached material as shown. I will include acknowledgments and/or appropriate citations to your work as shown and copyright and reprint rights information in a special appendix. The bibliographical citation will appear at the end of the manuscript as shown. Please advise me of any changes you require.

Please indicate your approval of this request by signing in the space provided, attaching any other form or instruction necessary to confirm permission. If you charge a reprint fee for use of your material, please indicate that as well. If you have any questions, please call me at the number above.

I hope you will be able to reply immediately. If you are not the copyright holder, please forward my request to the appropriate person or institution.

Thank you for your cooperation,

Troy R. Munro

I hereby give permission to Troy R. Munro to reprint the requested article in his thesis, with the following acknowledgment:

Munro, T.R., Koeln, J.P., Fassmann, A.W., Barnett, R.J., and Ban, H., 2012, "Surface Geometry Effect on Bubble Onset in Microgravity Pool Boiling," Manuscript submitted for publication to International Journal of Heat and Mass Transfer.

Signed: 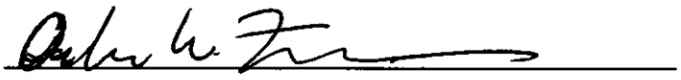

Date: 2/26/2012

Fee: —

Troy R. Munro
21 Aggie Vlg Apt C
Logan, UT 84341
801-558-4780

To Whom It May Concern:

As part of my thesis in the Department of Mechanical and Aerospace Engineering at Utah State University, I have used two papers that have been submitted to Journal of Heat Transfer and the International Journal of Heat and Mass Transfer. To include these papers in my thesis I need the permission of each coauthor on each paper, but one of the coauthors (Robert J. Barnett) has passed away on December 30, 2011, and is unable to give his permission. We regret his loss and as such, this thesis is dedicated in part to Rob.

Sincerely,

Troy R. Munro

APPENDIX B. ADDITIONAL INFORMATION

RADIATION CONTRIBUTION CALCULATION

To investigate the contribution of radiation heat transfer to the overall heat transfer of the system, a perturbation solution was developed, based on Eq. (1).

$$\frac{\partial^2 T}{\partial r^2} + \frac{1}{r}\frac{\partial T}{\partial r} + \frac{q'''}{k} = \frac{1}{\alpha}\frac{\partial T}{\partial t} \tag{1}$$

The process of this perturbation method was to non-dimensionalize the equation to find the small perturbation parameter, ε in Eq. (2).

$$\varepsilon = \frac{e\sigma r_0 T_\infty^3}{k} \tag{2}$$

The non-dimensional equation and boundary conditions are then perturbed resulting in Eq. (3), and after expansion, the ε terms .are collected and each equation of different orders of ε are solved by separation of variables.

$$\frac{\partial^2}{\partial \xi^2}(\theta_0 + \varepsilon\theta_1 + \varepsilon^2\theta_2) + \frac{1}{\xi}\frac{\partial}{\partial \xi}(\theta_0 + \varepsilon\theta_1 + \varepsilon^2\theta_2) + \frac{q'''r_0^2}{kT_\infty} = \frac{1}{\alpha}\frac{\partial}{\partial \tau}(\theta_0 + \varepsilon\theta_1 + \varepsilon^2\theta_2) \tag{3}$$

The perturbation solution is given in Eq. (4), where the Biot number is $Bi = hr_0/k$, and the equation was solved with a numerical integration with the results showing that radiation heat transfer is less than 0.1% and can be considered negligible.

$$\frac{T}{T_\infty} = -\frac{q'''r^2}{4kT_\infty} + \frac{q'''r_0^2}{2kT_\infty Bi} + 1 + \frac{q'''r_0^2}{4kT_\infty} + \sum_{k=1}^{\infty} a_{k0} J_0\left(\lambda_{ko}\frac{r}{r_0}\right)\exp\left(-\lambda_{ko}^2\frac{\alpha^2 t}{r_0^2}\right) + \varepsilon\left[1 - \left(1 + \frac{q'''r_0^2}{2kT_\infty Bi}\right)^4 - \left[\sum_{k=1}^{\infty} a_{k0} J_0\left(\lambda_{ko}\frac{r}{r_0}\right)\exp\left(-\lambda_{ko}^2\frac{\alpha^2 t}{r_0^2}\right)\right]^4 + \sum_{k=1}^{\infty} a_{k1} J_0\left(\lambda_{k1}\frac{r}{r_0}\right)\exp\left(-\lambda_{k1}^2\frac{\alpha^2 t}{r_0^2}\right)\right] \tag{4}$$

Where a_{k0} is given by Eq. (5), a_{k1} is given by Eq. (6), λ_{k0} is the root of Eq. (7), and λ_{k1} is the root of Eq. (8).

$$a_{k0} = \frac{\frac{q'''r_0^2}{2kT_\infty\lambda_{ko}}J_0(\lambda_{ko}) - \left(\frac{q'''r_0^2}{2Bi kT_\infty\lambda_{ko}} + \frac{q'''r_0^2}{kT_\infty\lambda_{ko}}\right)J_1(\lambda_{ko})}{\frac{(Bi^2+\lambda_{k0}^2)J_0^2(\lambda_{ko})}{2\lambda_{k0}^2}} \tag{5}$$

$$a_{k1} = \frac{\int_0^1 \left(\left[-1 + \left(1 + \frac{q''' r_0^2}{2kT_\infty Bi} \right)^4 + \left(\sum_{k=1}^{\infty} a_{k0} J_0\left(\lambda_{ko} \frac{r}{r_0} \right) \right)^4 \right] J_0\left(\lambda_{k1} \frac{r}{r_0} \right) \right) d\frac{r}{r_0}}{\int_0^1 \frac{r}{r_0} J_0^2\left(\lambda_{k1} \frac{r}{r_0} \right) d\frac{r}{r_0}} \quad (6)$$

$$Bi \mathrm{J}_0(\lambda_{\mathrm{ko}}) = \lambda_{\mathrm{ko}} \mathrm{J}_1(\lambda_{\mathrm{ko}}) \quad (7)$$

$$Bi \mathrm{J}_0(\lambda_{\mathrm{k1}}) = \lambda_{\mathrm{k1}} \mathrm{J}_1(\lambda_{\mathrm{k1}}) \quad (8)$$